

# One-dimensional model for QCD at high energy

E. Iancu <sup>a,1,2</sup>, J.T. de Santana Amaral <sup>b,1</sup>, G. Soyez <sup>a,1,3</sup>,  
D.N. Triantafyllopoulos <sup>c,1</sup>

<sup>a</sup> *Service de Physique Théorique de Saclay, CEA/DSM/SPhT, F-91191 Gif-sur-Yvette, France*

<sup>b</sup> *Instituto de Física, Universidade Federal do Rio Grande do Sul, 91501 Porto Alegre (RS), Brazil*

<sup>c</sup> *ECT\*, Villa Tambosi, Strada delle Tabarelle 286, I-38050 Villazzano (TN), Italy*

---

## Abstract

We propose a stochastic particle model in (1+1)-dimensions, with one dimension corresponding to rapidity and the other one to the transverse size of a dipole in QCD, which mimics high-energy evolution and scattering in QCD in the presence of both saturation and particle-number fluctuations, and hence of Pomeron loops. The model evolves via non-linear particle splitting, with a non-local splitting rate which is constrained by boost-invariance and multiple scattering. The splitting rate saturates at high density, so like the gluon emission rate in the JIMWLK evolution. In the mean field approximation obtained by ignoring fluctuations, the model exhibits the hallmarks of the BK equation, namely a BFKL-like evolution at low density, the formation of a traveling wave, and geometric scaling. In the full evolution including fluctuations, the geometric scaling is washed out at high energy and replaced by diffusive scaling. It is likely that the model belongs to the universality class of the reaction-diffusion process. The analysis of the model sheds new light on the Pomeron loops equations in QCD and their possible improvements.

---

<sup>1</sup> *E-mail addresses:* iancu@dsm-mail.cea.fr (E. Iancu), thiago.amaral@ufrgs.br (J.T. de Santana Amaral), gsoyez@dsm-mail.cea.fr (G. Soyez), dionysis@ect.it (D.N. Triantafyllopoulos).

<sup>2</sup> Membre du Centre National de la Recherche Scientifique (CNRS), France.

<sup>3</sup> On leave from the Fundamental Theoretical Physics group of the University of Liège.

## 1 Introduction

Much of the recent progress towards understanding the dynamics of QCD at high energies comes from the observation [1, 2] that the QCD evolution (at least, in its ‘leading–logarithmic approximation’ with respect to the energy logarithm  $\ln s$ ) is a relatively simple classical stochastic process in the universality class of the ‘reaction–diffusion process’.

In its canonical formulation (see, e.g., Refs. [3, 4]), the reaction–diffusion process  $A \rightleftharpoons AA$  involves particles of type  $A$  located at the sites of an infinite, one–dimensional, lattice, which are endowed with the following dynamics: a particle can locally split into two ( $A \rightarrow AA$ ), two particles can recombine into one ( $AA \rightarrow A$ ), and a particle can diffuse from one site to the adjacent sites. But the associated *universality class* covers a wide variety of stochastic processes, whose detailed microscopic dynamics can be different from those of the ‘canonical’ realization described above, but which share the same basic ingredients, leading to an *effective* one–dimensional dynamics with local growth and diffusion in the dilute regime, saturation of the occupation numbers at high density, and fluctuations in the particle number. These ingredients appear to be sufficient to ensure a *universal* behaviour for all such processes in specific limits (large time, weak noise), as empirically demonstrated by the experience with a large number of models [4], and conceptually understood from general arguments [5, 6].

In particular, in the context of high–energy QCD, the ‘particles’ correspond to gluons (or dipoles), the ‘time’ axis corresponds to the rapidity  $Y \sim \ln s$ , and the one–dimensional ‘spatial’ axis is the logarithm of the gluon transverse momentum (or the dipole transverse size). Furthermore, the ‘particle splitting’ corresponds to the BFKL evolution [7, 8], the ‘recombination’, to the non–linear effects responsible for gluon saturation [9–16], and the ‘diffusion’, to the non–locality of the BFKL kernel and the various gluon, or dipole, vertices in the transverse space. Of course, the actual QCD problem is much more complicated than just particle splitting and merging: it involves color degrees of freedom, whose role appears to be irreducible at high density; also, gluon saturation (as described by the JIMWLK equation [14–16]) does not occur via ‘mechanical’ recombination, but rather as a consequence of coherent, strong field, effects [17]; besides, the transverse plane has two dimensions and, moreover, the theoretical descriptions typically involve two types of transverse coordinates — the transverse size (or momentum) and the position in impact parameter space —, so the relevant transverse phase–space is truly four–dimensional. In spite of this, one can argue that, under suitable approximations, the dominant high–energy dynamics at fixed impact parameter is indeed one–dimensional, with the relevant dimension being the transverse size (or momentum), as alluded to above [1, 2].

The universality of the reaction–diffusion process is especially interesting in this QCD context, since in spite of considerable work and progress over the recent years [1, 2, 12–27], a complete theory for the high–energy evolution and scattering in QCD is still lacking. Moreover, even the approximate versions of this theory that are currently known, like the ‘Pomeron loop’ equations proposed in Refs. [2, 20, 21, 24], or the ‘self–dual’ [23] effective Hamiltonian of Refs. [26, 27], appear to be too complicated to deal with in practice, and may also suffer from internal inconsistencies [28]. In view of this, it is particularly rewarding that some fundamental aspects of QCD at high energy, like the asymptotic behaviour of the scattering amplitudes (in particular, the breakdown of ‘geometric’ scaling [29–33] and the emergence of a new, ‘diffusive’, scaling at very high energies), could have been inferred from the correspondence with the reaction–diffusion process in statistical physics [1, 2, 6, 34–37].

But this correspondence has its own, rather strong, limitations, which could be overcome only through deeper investigations of the actual, microscopic, dynamics. In view of the difficulty to perform such studies directly in QCD, one nowadays assists at a regain of interest in *stochastic particle models* [34, 35, 38–43], which aim at simulating the ‘Pomeron loops dynamics’ — by which we mean the high-energy evolution and scattering in the presence of both saturation and particle-number fluctuations — in lower dimensions (zero or one transverse dimensions). Such models are interesting not only because they allow for explicit solutions (even analytic ones, in the case of zero dimensions [40–43]), and thus permit us to familiarize ourselves with the physical consequences of the Pomeron loops, but also because they provide explicit evolution equations, and thus give us some insight into the structural aspects that one should expect in QCD. Besides, if sufficiently rich, a model may also allow us to study *non-universal* aspects, like the influence of the initial conditions at low energy, or the details of the transition from geometric to diffusive scaling.

However, in order to meet with these desiderata a model should contain as much as possible of the actual QCD dynamics, to the extent that this can be made consistent with the limitations inherent in the model (like its low dimensionality and the lack of color degrees of freedom). For instance, the model should respect general symmetry properties, like the *boost-invariance* of the evolution equations, which in fact is one of the main physical arguments in favour of Pomeron loops [19, 23, 24, 44]. (This condition is sometimes reformulated as the ‘self-duality’ of the evolution Hamiltonian [23, 24, 26].) Also, the model should incorporate some general properties of QCD at high energy, like the fact that a particle which scatters off a dense system undergoes *multiple scattering*. Moreover, in the limiting cases where the QCD equations are presently known, the model should reproduce suitable versions of these equations: it should be similar to the QCD dipole picture [8, 44] in the dilute regime, and it should reduce to a suitable version of the BK equation, or of the Balitsky–JIMWLK hierarchy<sup>4</sup> [12–16], in the high-density regime where the particle-number fluctuations become unimportant.

Together, the above conditions turn out to be very constraining, and it is not so easy to construct a model which fulfills all these constraints. In fact, most of the models proposed so far are directly inspired by the canonical reaction–diffusion process [34, 35, 38–41, 43] (which is also closely related [43] to the old ‘Reggeon field theory’) and as such, not only they cannot be used to study deviations from universality, but also they have difficulties to accommodate multiple scattering: to be consistent with boost-invariance, such models must assume that a projectile particle can undergo only single scattering, however dense the target is.

A noticeable exception in that sense is a zero-dimensional model originally proposed by Mueller and Salam [45], in an attempt to include saturation effects in the dipole picture, which has been recently reconsidered in Ref. [42] (see also Ref. [46]). In this model, boost-invariance and multiple scattering (in the eikonal approximation) are used as building principles, and it turns out that — due to simplifications associated with the lack of transverse dimensions — these two conditions are almost enough to uniquely fix the evolution law. The only additional assumption, which is fully consistent with the known situation in QCD, is that the evolution proceeds via particle splitting *alone* (no recombination), with one new particle being emitted per unit rapidity. Remarkably, the particle emission rate which emerges from these constraints is

---

<sup>4</sup> One should perhaps recall at this point that the BK equation and the Balitsky hierarchy are essentially equivalent at large- $N_c$ , which is the limit of interest for the particle models.

*non-linear* in the number of preexisting particles and *saturates* at some maximal value when this number is large enough, as a consequence of multiple scattering. These features are appealing since rather similar to gluon saturation in the framework of the JIMWLK evolution.

But the lack of transverse dimensions greatly restricts the spectrum of physical problems that can be studied in the framework of the model: the only non-trivial problem which can be addressed in zero dimensions [42, 45] is that of the approach of the  $S$ -matrix towards the black disk limit  $S = 0$ . But the most interesting problems in the context of the high-energy evolution are those related to the coexistence of two regimes, one dense and one dilute (at low, and respectively, high transverse momenta), separated by the saturation momentum. In order to consider such problems one needs at least one transverse dimension — that expressing the gluon momentum, or the dipole size. It is our purpose in this paper to present an extension of the particle model in Refs. [42, 45] to one transverse dimension, denoted as  $x$ , to be eventually identified — in the correspondence with QCD — to the logarithm of the inverse size of a dipole:  $x \leftrightarrow \ln(r_0^2/r^2)$ , where  $r$  is the generic dipole size and  $r_0$  is some arbitrary scale of reference (typically, the size of the dipole which started the evolution at  $Y = 0$ ).

The model that we shall consider is constrained by the same physical assumptions as in Refs. [42, 45] — boost-invariance, multiple scattering and evolution via particle splitting —, but in the presence of the transverse dimension these assumptions are not sufficient anymore to completely fix the dynamics. Yet, as we shall see, they strongly constrain this dynamics: the only non-trivial (class of) solution(s) to these constraints that we shall find is the one which appears as the natural, although not necessarily obvious, generalization of the original model in zero dimensions. Specifically, the elementary particle-particle scattering amplitude is now *non-local* in  $x$ , although very *short-ranged*, corresponding to the fact that QCD favors the interaction between dipoles with similar sizes. Accordingly, the rate for particle emission at a particular site  $x$  (i.e., for emitting dipoles of a given size  $r$ ) is found to be proportional to the scattering amplitude between the new particle and the preexisting ones, and thus it depends upon the occupation numbers  $n(y)$  at all the other sites  $y$ . Once again, this emission rate saturates at its maximal value when the occupation numbers at the site of interest, or in its vicinity, become large enough.

The one-dimensional model endowed with this dynamics develops a very interesting structure, which is formally similar to that of the corresponding model in zero dimensions [42], but whose physical consequences are considerably richer, and also much closer to QCD. The evolution Hamiltonian<sup>5</sup>, which is self-dual (as it should, given the built-in boost-invariance), can be recognized as an extension of the JIMWLK Hamiltonian which allows for particle-number fluctuations. The equations for the scattering amplitudes generated by this Hamiltonian provide an intuitive generalization of the Balitsky-JIMWLK hierarchy in which the projectile and the target are symmetrically treated. The general structure of these equations is in fact similar to that of the ‘Pomeron loop equations’ proposed in QCD at large  $N_c$  [2, 20, 21], in the sense of including three types of terms: linear terms responsible for the BFKL evolution, source terms describing particle-number fluctuations in the target (or, equivalently, saturation effects in the projectile), and non-linear terms corresponding to saturation effects in the target, which ensure the unitarization of the scattering amplitudes at high energy.

---

<sup>5</sup> In the context of a stochastic particle model, a Hamiltonian can be identified by rewriting the master equation in operator form; see Sect. 2 below for details.

At the same time, some interesting differences are found between the structure of the fluctuation terms in the toy–model equations and, respectively, the ‘Pomeron loop’ equations in QCD, which invites us to a more careful comparison between these two sets of equations. This study (to be detailed in the Appendix) shows that the observed differences reflect different ways to organize perturbation theory in the weak scattering regime, which are essentially equivalent, in the sense of providing the same dominant behaviour at high energy. This being said, the toy–model equations appear to be more symmetric in their treatment of the target versus projectile, and it is likely that a similar symmetry should hold in the complete equations of QCD, for which the toy model provides some inspiration.

Furthermore, the presence of a transverse dynamics in the toy model allows for explicit comparisons with the corresponding dynamics in QCD and, more generally, for studies of the universality. It appears that the linearized version of the toy–model equations (as appropriate in the dilute regime) is very close to the BFKL dynamics, whereas the mean–field version of the same equations (in which the expectation values are assumed to factorize) is similarly close to the BK dynamics. Namely, in the dilute regime, the solution shows the characteristic BFKL pattern [7] (exponential increase in  $Y$ , exponential decrease in  $x$  with some ‘anomalous dimension’, diffusion in  $x$  with diffusive radius  $\propto \sqrt{Y}$ ), and even approaches ‘color transparency’ at very large values of  $x$ . After including non–linear terms in the mean–field approximation, one observes saturation, the formation of a traveling wave, and geometric scaling — all that being indeed very similar to QCD [30, 31, 33].

A stochastic particle model with the linear and mean–field behaviour aforementioned is expected to belong to the universality class of the reaction–diffusion process, and this will be indeed confirmed by a numerical study of our model: the position of the traveling fronts (the toy–model analog of the logarithm of the saturation momentum) is thus found to be a random quantity with a dispersion increasing linearly with  $Y$ , and the shape of the average amplitude is seen to approach diffusive scaling at very large  $Y$ . Our present numerical analysis is only exploratory — it is merely intended to verify the universal features of the dynamics —, but we plan to perform a more detailed such a study in a further publication, and thus also study some non–universal aspects.

To summarize, although conceptually rich and relatively close to QCD (at least, in the limiting cases in which the comparison is possible), the model that we shall introduce here remains relatively simple and allows for systematic studies, including numerical ones. This model could therefore serve as a playground for testing new ideas concerning either the formal structure of the high–energy evolution equations in QCD, or the effects of the evolution with Pomeron loops on various physical processes.

The paper is organized as follows: In Sect. 2 we shall describe the construction of the model from the underlying physical assumptions, present the master equation for the probabilities, and discuss some of its general properties. In Sect. 3, we shall use the master equation to deduce evolution equations for physical observables, like the  $k$ –body particle densities and the scattering amplitudes. Then, in Sect. 4, we shall present an analytic study of these equations, which will successively focus on the linear approximation, the mean–field approximation, and the qualitative aspects of the full evolution with fluctuations. These analytic considerations will be then illustrated by the numerical results in Sect. 5, which will also substantiate our expectation that the model should belong to the universality class of the reaction–diffusion process. Finally, Sect. 6 contains our conclusion and a brief account of the analysis in the Appendix.

## 2 Construction of the model

In this section, we shall formulate our stochastic particle model for high-energy evolution and scattering in QCD. As explained in the Introduction, this is a  $(1 + 1)$ -dimensional model, where one of the dimensions refers to the rapidity  $Y$  (the logarithm of the energy), which plays the role of a ‘time’ for the high-energy evolution, while the other one is a spatial dimension — the position of the particle along an infinite one-dimensional axis. For the analogy with QCD, one should keep in mind that this spatial dimension corresponds to a *size* in QCD, more precisely to the logarithm of the inverse of the transverse size of a dipole. For the sake of the presentation, we shall first describe the discretized version of the model, where the spatial dimension is assimilated to a one-dimensional lattice, with lattice points labeled by  $i$ . This is, of course, also the version of the model which is best suited for the numerical implementation to be eventually discussed. However, as we shall later demonstrate, the continuum limit of the model is well-defined and rather straightforward to obtain.

A *system* of particles is then defined by specifying the number of particles  $n_i$  (or ‘occupation numbers’) at all the sites of the lattice (some of these sites could be empty). With increasing rapidity, the composition of the system can randomly vary, via particle splitting according to a law to be shortly specified. Hence, the particle distribution is stochastic, and the state of the system at rapidity  $Y$  is described by the probability  $P(\{n\}, Y)$  to find a given configuration  $\{n\} \equiv \{\dots, n_i, n_{i+1}, \dots\}$  of particles.

In order to mimic a scattering problem, we shall consider two types of particles, say particles of type ‘right’ ( $R$ ) and particles of type ‘left’ ( $L$ ), which coexist at the lattice sites and interact with each other via generally non-local interactions (see below for details). The particle labels ‘ $R$ ’ and ‘ $L$ ’ refer, of course, to the fact that in an actual scattering problem, the two colliding systems propagate in opposite directions along the collision axis<sup>6</sup>.

In what follows, we shall assume that the average  $S$ -matrix element for the elastic scattering can be given the factorized form

$$\langle S \rangle_Y = \sum_{\{n\}, \{m\}} P_R(\{n\}, Y - Y_0) P_L(\{m\}, Y_0) \mathcal{S}(\{n\}, \{m\}), \quad (2.1)$$

where  $Y$  is the total rapidity separation between the two systems and is divided between the ‘target’ (the right mover), which has a rapidity  $Y - Y_0$  in the chosen frame, and the ‘projectile’ (the left-mover), which has a rapidity  $-Y_0$  (with  $Y_0 > 0$ ). Furthermore,  $P_R(\{n\}, Y - Y_0)$  and  $P_L(\{m\}, Y_0)$  are probability distributions describing the two systems at the time of scattering, and  $\mathcal{S}(\{n\}, \{m\})$  is the  $S$ -matrix for the elastic scattering between two given configurations  $\{n\}$  and  $\{m\}$  of the target and, respectively, the projectile. Finally, the sum in Eq. (2.1) runs over all the possible configurations in both systems.

A factorization similar to Eq. (2.1) is known to hold in QCD for onium–onium scattering within the dipole picture [44, 47]. More generally, such a factorization emerges from a more fundamental, quantum, description in terms of light-cone wavefunctions whenever the single-particle states are eigenstates of the  $S$ -matrix operator (which is our implicit assumption here).

---

<sup>6</sup> One should not confound this collision axis with the spatial dimension in the toy model, which rather corresponds to transverse degrees of freedom in QCD, as explained before.

On physical grounds, the average  $S$ –matrix must be independent of the rapidity divider  $Y_0$ , i.e., upon the choice of a Lorentz frame, which implies (with short–handed notations):

$$0 = \frac{d\langle S \rangle}{dY_0} = \sum_{\{n\},\{m\}} \left( P_R(Y - Y_0) \frac{\partial P_L(Y_0)}{\partial Y_0} + \frac{\partial P_R(Y - Y_0)}{\partial Y_0} P_L(Y_0) \right) \mathcal{S}(\{n\}, \{m\}). \quad (2.2)$$

This condition, which relates properties of the scattering to those of the evolution with  $Y$ , represents a rather strong constraint on the latter, and can be even used to fix the structure of the evolution law under some additional assumptions. Let us enumerate here the main assumptions that we shall rely on in that respect:

- (i) *Multiple scattering in the eikonal approximation.* Let  $\sigma_{ij} = 1 - \tau_{ij}$  denote the  $S$ –matrix describing the scattering between two elementary particles with positions  $i$  and  $j$ ; here,  $\tau_{ij}$  is the corresponding  $T$ –matrix and is assumed to be real, as expected for the dominant behaviour at high energy. Each particle from the target can scatter off all the particles in the projectile, and different particles from the target scatter independently off each other. Then, the  $S$ –matrix for given configurations of the target and the projectile reads:

$$\mathcal{S}(\{n\}, \{m\}) = \prod_{i,j} \sigma_{ij}^{n_i m_j}. \quad (2.3)$$

- (ii) *One particle emission per evolution step.* We shall assume that, when increasing rapidity in one step ( $Y \rightarrow Y + dY$ ), the evolution consists in the emission of a single additional particle, with a probability which generally depends upon all the occupation numbers in the system. That is, the additional particle is emitted *coherently* from all the previous ones.

Both these assumptions are natural from the perspective of perturbative QCD at high energy: The eikonal approximation is the standard method to resum multiple scattering in QCD at high–energy, for both gluons (see, e.g., Refs. [12, 14, 15]) and dipoles [8, 13, 44]. Furthermore, the high–energy QCD evolution in the leading logarithmic approximation consists indeed in the emission of a single  $s$ –channel gluon at each step of the evolution. Note that, unlike other models in the literature [39–41, 43], our model does not include a mechanism for particle recombination, in agreement with the fact that there is no ( $s$ –channel) gluon, or dipole, recombination in QCD in the leading–logarithmic approximation. Rather, as we shall see, particle saturation occurs via high–density effects in the emission rate, similar to the gluon saturation in the framework of the JIMWLK evolution [17].

In zero (transverse) dimensions, that is, for a model living at a single lattice site, the assumptions (i–ii) above are sufficient to completely fix — via the condition (2.2) for boost invariance — the structure of the evolution equation for the probabilities  $P$  [42, 45]. But with one spatial dimension at our hand, there is still much freedom left, because one can make different choices for the non–locality of the splitting process. As we shall see in what follows, a relatively simple model which is conceptually interesting (in the sense of bearing many similarities to QCD) can be obtained after also imposing the following, third, constraint:

- (iii) *After one step in the evolution, the configuration of the system changes only by the addition of one new particle at some arbitrary site.* That is, the configuration remains the same as prior to the evolution except for the presence of the additional particle. This is clearly a stronger constraint than the above assumption (ii) which would allow for any final state

with one additional particle as compared to the original state, irrespective of the spatial distribution of the particles in the final state.

Under this additional assumption, the evolution equation for  $P(\{n\}, Y)$  (the ‘master equation’) takes the following generic form:

$$\frac{\partial P(\{n\}, Y)}{\partial Y} = \sum_i \left[ f_i(\dots, n_i - 1, \dots) P(\dots, n_i - 1, \dots, Y) - f_i(\{n\}) P(\{n\}, Y) \right], \quad (2.4)$$

where the quantity  $f_i(\{n\})$  has the meaning of a ‘deposit’ rate: this is the probability per unit rapidity to find an extra particle at site  $i$  after one step of the evolution, starting from an original configuration  $\{n\}$ . The positive (gain) term in the r.h.s. Eq. (2.4) shows that in order to arrive at a final configuration  $\{n\}$  after one step in this evolution, one needs to start in a configuration containing one particle less on the site  $i$ , where  $i$  is arbitrary. The negative (loss) term is necessary for the conservation of the probability.

The evolution law in Eq. (2.4) deserves some physical discussion. But let us first complete the construction of the model, by deducing an explicit form for the deposit rate  $f_i(\{n\})$ . As anticipated, this is obtained by exploiting the condition of boost–invariance, that is, by inserting the generic master equation (2.4) into Eq. (2.2), to deduce the following constraint :

$$\sum_i [f_i(\{n\}) t_i(\{m\}) - f_i(\{m\}) t_i(\{n\})] = 0, \quad (2.5)$$

where we have defined

$$t_i(\{n\}) = 1 - \prod_j \sigma_{ij}^{n_j}. \quad (2.6)$$

The above notation is not accidental, since  $t_i(\{n\})$  is formally equal to the amplitude for the scattering of a projectile particle at site  $i$  off a target with a given configuration  $\{n\}$ . The most general solution to Eq. (2.5) that we have found reads

$$f_i(\{n\}) = \sum_j c_{ij} t_j(\{n\}) \quad \text{with} \quad c_{ij} = c_{ji}, \quad (2.7)$$

and where  $c_{ij}$  is independent of the particle occupation numbers. It is convenient to choose  $c_{ij} \propto \delta_{ij}$ , since this leads to a relatively simple and intuitive model which still has a rather rich structure, as we shall later see. Namely, we shall fix our model by choosing

$$c_{ij} = \frac{\Delta}{\tau} \delta_{ij}, \quad (2.8)$$

where  $\tau \equiv \tau_{ii}$  and  $\Delta$  stands for the “lattice spacing” along the discretized spatial axis. The fact that  $c_{ij}$  is proportional to  $\Delta$  is natural, since the deposit rate density  $f_i/\Delta$  will be well-defined in the continuum limit  $\Delta \rightarrow 0$ . The fact that we choose  $c_{ij}$  proportional to  $1/\tau$  is again natural, since in the low density limit  $f_i$  should be of order  $\mathcal{O}(1)$  when measured in units of  $\tau$ . Indeed, when the  $n_j$ ’s are relatively small, such that  $n_j \tau_{ij} \ll 1$ , the scattering amplitude  $t_i$  in Eq. (2.6) reduces to  $t_i \approx \sum_j \tau_{ij} n_j$  and therefore the particular parametric dependence of  $c_{ij}$  on  $\tau$  exhibited above is clearly necessary for the condition to be fulfilled.

To conclude, as a result of the various assumptions presented above, we finally arrive at the model defined by the master equation (2.4) with the following expression for the deposit rate :

$$\frac{f_i(\{n\})}{\Delta} = \frac{1 - \prod_j \sigma_{ij}^{n_j}}{\tau} = \frac{t_i(\{n\})}{\tau}. \quad (2.9)$$

Up to an overall normalization, this is simply the scattering amplitude for the scattering between the particle newly produced at site  $i$  and the preexisting particles in the system, from which the new particle has been emitted.

To better appreciate the physical content of the above formula, we need to know a little bit more about the elementary scattering amplitude  $\tau_{ij}$ . Later on, we shall present an explicit model for this quantity, dictated by the analogy with QCD (see Sect. 4 for details). Here, it suffices to mention that  $\tau_{ij}$  depends only upon the separation  $|i - j|$  and is rapidly decreasing when increasing this separation. In particular, the quantity  $\tau \equiv \tau_{ii}$  is independent of  $i$  (a property that has been already used in writing Eq. (2.8)) and will be taken to be small:  $\tau \ll 1$  (the analogous quantity in QCD is of  $\mathcal{O}(\alpha_s^2)$ ). One therefore has  $\tau_{ij} \ll 1$  for any pair  $(ij)$ .

Armed with this knowledge, we now return to Eq. (2.9) and discuss some limiting cases:

(i) When the occupation numbers are relatively small, such that  $n_j \ll 1/\tau_{ij}$ , one can expand  $\sigma_{ij}^{n_j} \approx 1 - n_j \tau_{ij}$ , and then the deposit rate density for the given site  $i$  becomes simply proportional to the particle occupation numbers at all sites:

$$\frac{f_i(\{n\})}{\Delta} \approx \sum_j \frac{\tau_{ij}}{\tau} n_j \quad \text{when } n_j \ll 1/\tau_{ij} \text{ for any } j. \quad (2.10)$$

This describes a situation where the extra particle at  $i$  is *incoherently* emitted by any of the preexisting particles in the system. When the approximation (2.10) holds for *any* site  $i$ , we shall speak about the *dilute*, or *linear*, regime. Since, as mentioned before,  $\tau_{ij}$  is a decreasing function of the separation  $|i - j|$ , the dilute regime is realized when *all* the occupation numbers obey the condition  $n_j \ll 1/\tau$ . The dipole picture in QCD [8] is the right term of comparison for our toy model in this dilute regime; and, indeed, if one computes the analogous deposit rate in the dipole picture, one finds that this is linear in the dipole density [44].

(ii) When at least one of the occupation numbers  $n_j$  becomes so large that  $\sigma_{ij}^{n_j} \ll 1$  (this requires  $n_j \gtrsim 1/\tau_{ij}$ ), the deposit rate at  $i$  saturates at its maximal value of  $\mathcal{O}(1/\tau)$  :

$$\frac{f_i(\{n\})}{\Delta} \approx \frac{1}{\tau} \quad \text{when } n_j \gtrsim 1/\tau_{ij} \text{ for some } j. \quad (2.11)$$

In particular, a sufficient condition to have saturation at a given site  $i$  is that the respective occupation number  $n_i$  obeys  $n_i \gtrsim 1/\tau$ . This is again similar to the situation in QCD, where the gluon emission rate in the JIMWLK equation (the analog of the deposit rate in the toy model) saturates when the gluon occupation numbers are sufficiently high.

One may also notice that in the limit where the scattering is truly local,  $\tau_{ij} = \tau \delta_{ij}$ , Eq. (2.9) yields  $f_i/\Delta = (1 - \sigma^{n_i})/\tau$ , with  $\sigma \equiv 1 - \tau$ . In this limit, the different lattice sites decouple from each other, and each of them evolves according to the zero-dimensional model of Refs. [42,45]. This limit is uninteresting for the present purposes, and shall not be considered anymore.

Let us now return, as promised, to a physical discussion of the evolution described by Eq. (2.4). To that aim, it is useful to imagine a specific microscopic mechanism leading to

this evolution. It is natural to assume that the process leading to the production of the extra particle in one evolution step is the splitting of one particle into two new ones. For this mechanism to be consistent with Eq. (2.4), one additional assumption is however needed: at least one of the two daughter particles produced after such a splitting must remain on the same lattice site as its parent particle. Introducing the emission rate  $g_{j \rightarrow ji}(\{n\})$  for a particle at  $j$  to split into two particles at  $j$  and  $i$ , respectively, with arbitrary  $i$ , we are lead to the following master equation

$$\frac{\partial P(\{n\}, Y)}{\partial Y} = \sum_{ij} \left[ g_{j \rightarrow ji}(\dots, n_i - 1, \dots) P(\dots, n_i - 1, \dots, Y) - g_{j \rightarrow ji}(\{n\}) P(\{n\}, Y) \right], \quad (2.12)$$

which leads to Eq. (2.4) after identifying  $f_i(\{n\}) = \sum_j g_{j \rightarrow ji}(\{n\})$ . The process in Eq. (2.12) is quite peculiar in the sense that the particle which splits does not disappear in the final state, rather it gets replaced by a new particle at the same site<sup>7</sup>. In the analogy with QCD — in which, we recall, particle positions correspond to dipole sizes —, this would correspond to a process in which a dipole of size  $j$  splits into two dipoles, one with the same size  $j$  and the other one with some arbitrary size  $i$ . This is quite different from the (BFKL) picture of dipole splitting in QCD at large  $N_c$  [8], where the daughter dipoles have generic sizes, which typically are comparable to the size of the parent dipole. But in spite of this explicit dissimilarity at the level of the physical interpretation, the toy model evolution generated by Eqs. (2.4) and (2.9) turns out to have many common features with the high-energy evolution in QCD, as it should become clear from the analysis in the subsequent sections.

Last, but not least, we notice that one can put the model in the Hamiltonian form

$$\begin{aligned} \frac{\partial P(\{n\}, Y)}{\partial Y} &= -\frac{\Delta}{\tau} \sum_i \left[ 1 - \exp \left( -\frac{\partial}{\partial n_i} \right) \right] \left[ 1 - \exp \left( \sum_j n_j \ln \sigma_{ij} \right) \right] P(\{n\}, Y) \\ &\equiv H P(\{n\}, Y), \end{aligned} \quad (2.13)$$

where the differential operator  $\exp(-\partial/\partial n_i)$  is the ‘translation’ operator which reduces the occupation number at site  $i$  by one:  $\exp(-\partial/\partial n_i) F(\dots, n_i, \dots) = F(\dots, n_i - 1, \dots)$  for a generic function  $F(\{n\})$ . This rewriting makes it explicit that the Hamiltonian underlying the evolution of the model is ‘self-dual’, that is, it is invariant under the self-duality transformation [23] which in the present context consists in exchanging

$$\frac{\partial}{\partial n_i} \longleftrightarrow - \sum_j n_j \ln \sigma_{ij}, \quad (2.14)$$

and then reversing the order of the operators. This self-duality is the expression of the constraint of boost-invariance on the structure of the evolution Hamiltonian [23, 24]. Thus, this condition is automatically fulfilled by our model, where boost-invariance is built-in. Also, the presence of two types of exponentials — one involving the particle occupation number and the other one, the derivative with respect to it — in Eq. (2.13) is reminiscent of the two types of Wilson lines which appear in the QCD Hamiltonian proposed in Refs. [26, 27]. In that case,  $\sum_j n_j |\ln \sigma_{ij}|$

<sup>7</sup> Incidentally, this discussion also shows that a natural generalization of the present model would be to allow for the more general splitting  $i \rightarrow jk$  with generic  $i$ ,  $j$ , and  $k$ , and with a rate  $g_{i \rightarrow jk}(\{n\})$ .

is replaced by the color field produced by the  $s$ –channel gluons, and  $\partial/\partial n_i$  by the (functional) derivative with respect to the color charge density of these gluons.

It is furthermore interesting to consider the approximate version of the master equation which is formally obtained by expanding the operator  $\exp(-\partial/\partial n_i)$  to linear order in the derivative:

$$\frac{\partial P(\{n\}, Y)}{\partial Y} \approx - \sum_i \frac{\partial}{\partial n_i} \left[ f_i(\{n\}) P(\{n\}, Y) \right]. \quad (2.15)$$

Less formally, this is simply the limit in which the difference between the two terms in the r.h.s. of Eq. (2.4) is assimilated to a derivative with respect to  $n_i$ , which is reasonable when  $n_i \gg 1$ , for any  $i$ . This is the limit of *large occupation numbers*, in which the fluctuations associated with the discreteness of the particle number become negligible.

In this limit, the self–duality of the evolution is of course lost, since the system property of being dense depends upon the frame. Moreover, it should be intuitively clear that, whatever frame we choose, the system cannot be dense at *all* the sites. Indeed, the spatial axis being infinite, there will always be an infinite number of sites where the occupation numbers are either zero, or small, of  $\mathcal{O}(1)$ , and this for any  $Y$ . Hence, Eq. (2.15) is merely a formal approximation, which for a given  $Y$  has, at most, a limited range of validity in  $x$  — it refers to the evolution of the *bulk* of the particles in a region with high occupancy.

This discussion is reminiscent of that of the JIMWLK equation in QCD, which has been established [14, 15] for systems with a relatively high gluon density and which ignores the fluctuations in the gluon number [2]. And, indeed, one can recognize the above equation (2.15) as the toy–model version of the JIMWLK equation. This analogy has been already discussed in the context of the zero–dimensional model in Ref. [42], to which we refer for more details. To summarize this section, the toy–model that we have here introduced reduces to (one–dimensional versions of the) dipole picture in the dilute regime and, respectively, to the JIMWLK picture in the regime of high occupancy, and in general it provides a self–dual ‘interpolation’ between these two pictures, as necessary for boost–invariance.

### 3 Evolution equations for the observables

Given the master equation (2.4) along with the deposit rate, Eq. (2.9), one can obtain the evolution equation for any ‘observable’  $\mathcal{O}$ , by which we shall mean a quantity whose event–by–event value  $\mathcal{O}(\{n\})$  depends upon the configuration  $\{n\}$  of the particles in the system. Its average value at rapidity  $Y$ , which is a measurable quantity, is given by

$$\langle \mathcal{O} \rangle_Y = \sum_{\{n\}} P(\{n\}, Y) \mathcal{O}(\{n\}). \quad (3.1)$$

Differentiating with respect to  $Y$  and performing a shift  $n_i - 1 \rightarrow n_i$  in the contributions arising from the gain (plus sign) terms in Eq. (2.4) one easily finds

$$\frac{\partial \langle \mathcal{O} \rangle_Y}{\partial Y} = \sum_i \left\langle f_i(\{n\}) \left[ \mathcal{O}(\dots, n_i + 1, \dots) - \mathcal{O}(\{n\}) \right] \right\rangle_Y. \quad (3.2)$$

In what follows, we shall specialize the generic evolution equation (3.2) to two interesting types of observables, namely, the  $k$ –body particle occupation numbers and the scattering amplitudes for projectiles made with a given number of particles. In the process, we shall also demonstrate that the continuum limit  $\Delta \rightarrow 0$  of the ensuing equations is well defined, and we shall furthermore compare these equations to the corresponding ones in QCD.

### 3.1 Particle number densities

The simplest observable that one can think of is  $\langle n_i \rangle_Y$  — the average occupation number at the site  $i$ . From Eq. (3.2), it is straightforward to obtain

$$\frac{\partial \langle n_i \rangle_Y}{\partial Y} = \left\langle \frac{\Delta(1 - \prod_j \sigma_{ij}^{n_j})}{\tau} \right\rangle_Y = \langle f_i(\{n\}) \rangle_Y, \quad (3.3)$$

with an obvious physical interpretation: the rate for the change in the average particle number at a given site is equal to the average value of the deposit rate at that particular site. Two limiting cases of Eq. (3.3) are particularly interesting, corresponding to the two limits of the deposit rate  $f_i$  discussed in relation with Eq. (2.10) and, respectively, Eq. (2.11) :

(i) If the system is relatively dilute ‘around the site  $i$ ’ — meaning that, for the typical configurations, one has  $n_i \ll 1/\tau$  and also  $n_j \ll 1/\tau$  for all the sites  $j$  which are not too far away from  $i$  —, then we can linearize  $\langle f_i \rangle_Y$  with respect to the (average) occupation numbers and thus obtain:

$$\frac{\partial \langle n_i \rangle_Y}{\partial Y} \approx \frac{\Delta}{\tau} \sum_j \tau_{ij} \langle n_j \rangle_Y. \quad (3.4)$$

In this regime, the particle occupation at site  $i$  and at the neighboring sites undergoes a *linear* evolution, leading to a rapid (exponential in  $Y$ ) rise in the respective average occupation numbers. This rapid rise, which will be explicitly demonstrated in Sect. 4, is the toy–model analog of the BFKL growth in the gluon (or dipole) distribution in QCD in the dilute regime [7].

(ii) If, on the other hand, the system is ‘dense at  $i$ ’, meaning that the average deposit rate  $\langle f_i \rangle_Y$  saturates at its maximum value, cf. Eq. (2.11), then the growth of the (average) occupation number at  $i$  is considerably slowed down:

$$\frac{\partial \langle n_i \rangle_Y}{\partial Y} \approx \frac{\Delta}{\tau}. \quad (3.5)$$

This equation shows that, once the particle occupation number at  $i$  becomes of  $\mathcal{O}(1/\tau)$ , its subsequent growth with  $Y$  is only very slow, *linear* in  $Y$ . This is the mechanism of *saturation* within the toy model, and is similar to gluon saturation in QCD, where the occupation numbers for the saturated modes grow also linearly with  $Y$  [17, 48, 49].

Returning to Eq. (3.3), one should also notice that this is not a closed equation for  $\langle n_i \rangle_Y$ , but rather the beginning of a *hierarchy* : if one expands  $\sigma_{ij}^{n_j} = \exp\{n_j \ln \sigma_{ij}\}$  in powers of  $n_j$  inside the brackets in the r.h.s., one generates  $k$ –body correlations of the occupation numbers with any  $k \geq 1$ . This invites us to consider the evolution equations obeyed by the general, ‘normal–ordered’,  $k$ –body occupation numbers, defined as

$$n_{i_1 \dots i_k}^{(k)} \equiv n_{i_1}(n_{i_2} - \delta_{i_1 i_2}) \dots (n_{i_k} - \delta_{i_1 i_k} - \dots - \delta_{i_{k-1} i_k}). \quad (3.6)$$

Here, the ‘normal ordering’ refers to the subtraction of  $\delta$ -functions, as explicit in the equation above, which are needed to guarantee that, in constructing  $n^{(k)}$ , one counts only sets of  $k$  particles which are all different from each other. The corresponding evolution equation can be readily obtained as

$$\frac{\partial \langle n_{i_1 i_2 \dots i_k}^{(k)} \rangle_Y}{\partial Y} = \sum_{j=1}^k \langle f_{i_j}(\{n\}) n_{i_1 i_2 \dots i_k}^{(k-1)} \rangle_Y, \quad (3.7)$$

where the notation  $i_j \not\in$  means that the  $i_j$  variable is to be omitted.

Before proceeding with the hierarchy for the scattering amplitudes, let us first briefly discuss the *continuum limit* of our model, which is straightforward. Clearly, this limit amounts to replacing  $i \rightarrow x_i = i\Delta$  and then letting  $\Delta \rightarrow 0$ , so that  $x_i \rightarrow x$ , with  $x$  our continuous spatial variable. Then, a sum over  $i$  gets converted into an integration over  $x$ :

$$\Delta \sum_i F_i \rightarrow \int dx F(x), \quad (3.8)$$

while a sum over all the possible configurations of the onium wavefunction becomes a path integral, that is

$$\sum_{\{n\}} \rightarrow \int [Dn(x)]. \quad (3.9)$$

The  $k$ -body (normal-ordered) particle *densities* are obtained from the corresponding occupation numbers after dividing by  $\Delta^k$  and then letting  $\Delta \rightarrow 0$ . For example, the 2-body, or pair, density is given by

$$n^{(2)}(x, y) = \lim_{\Delta \rightarrow 0} \left( \frac{n_i n_j}{\Delta^2} - \frac{\delta_{ij}}{\Delta} \frac{n_i}{\Delta} \right) = n(x) n(y) - \delta(x - y) n(x), \quad (3.10)$$

while the deposit rate density can be immediately obtained from Eq. (2.9), and reads

$$f(x) = \lim_{\Delta \rightarrow 0} \frac{f_i(\{n\})}{\Delta} = \frac{1 - \exp [\int dz n(z) \ln \sigma(x|z)]}{\tau} \equiv \frac{t(x)}{\tau}. \quad (3.11)$$

It is now straightforward to reexpress all the equations presented earlier in continuum notations. For instance, the 1-body and 2-body particle densities obey the following equations, as obtained by taking the continuum limit in Eqs. (3.3) and (3.7) (with  $k = 2$ ), respectively:

$$\frac{\partial \langle n(x) \rangle_Y}{\partial Y} = \langle f(x) \rangle_Y, \quad (3.12)$$

$$\frac{\partial \langle n^{(2)}(x, y) \rangle_Y}{\partial Y} = \langle f(x) n(y) + f(y) n(x) \rangle_Y. \quad (3.13)$$

It is important to notice that Eq. (3.13) has no singularities in the equal-point limit  $y = x$  thanks to the subtraction of the  $\delta$ -function in the definition (3.10) of the normal-ordered 2-body density. A similar property holds for the  $k$ -body densities with  $k > 2$ .

### 3.2 Scattering amplitudes: Beyond the Balitsky–JIMWLK equations

We now move to the scattering problem and start by assuming that the projectile consists in a single particle located at  $i$ . In QCD, this would correspond to a projectile made with a single dipole of size  $r_i \propto \exp(-x_i/2)$ . This implicitly means that we work in a frame in which almost all of the rapidity  $Y$  is carried by the target, whose wavefunction evolves according to Eqs. (2.4) and (2.9), whereas the rapidity of the projectile is so low that its evolution can be neglected. The  $S$ -matrix describing this scattering is obtained by replacing  $m_j \rightarrow \delta_{jk}$  in Eq. (2.3), which then yields  $s_k(\{n\}) = \prod_l \sigma_{lk}^{n_l}$ . By making use of Eq. (3.2), we deduce the following evolution equation

$$\frac{\partial \langle s_i \rangle_Y}{\partial Y} = \sum_j \frac{\Delta(1 - \sigma_{ij})}{\tau} \langle s_i s_j - s_i \rangle_Y , \quad (3.14)$$

which is not a closed equation — the average  $S$ -matrix element for the one-particle projectile being related to that for a projectile made with two particles —, but only the first equation in an infinite hierarchy. The general equation in this hierarchy can be obtained by studying the scattering of a projectile made with  $m$  particles, at given positions<sup>8</sup>  $i_1, i_2, \dots, i_m$ . For a given target configuration  $\{n\}$ , the corresponding  $S$ -matrix reads

$$s_{i_1} \dots s_{i_m} = \prod_{j_1} \sigma_{i_1 j_1}^{n_{j_1}} \dots \prod_{j_m} \sigma_{i_m j_m}^{n_{j_m}} = \prod_j (\sigma_{i_1 j} \dots \sigma_{i_m j})^{n_j} \quad (3.15)$$

and then Eq. (3.2) implies

$$\frac{\partial \langle s_{i_1} \dots s_{i_m} \rangle_Y}{\partial Y} = \sum_j \frac{\Delta(1 - \sigma_{i_1 j} \dots \sigma_{i_m j})}{\tau} \langle s_{i_1} \dots s_{i_m} s_j - s_{i_1} \dots s_{i_m} \rangle_Y . \quad (3.16)$$

Although obtained here by following the evolution of the target, these equations can be easily reinterpreted as describing evolution in the projectile. To that aim, it is important to notice that the kernel in the above equation, i.e. the quantity in front of the expectation value in the r.h.s., is precisely  $f_j(\{m\})$ , that is, the deposit rate at site  $j$  evaluated for the given configuration  $\{m\}$  of the *projectile*. Thus, Eq. (3.16) can be interpreted as follows: a splitting takes place in the projectile, leading to a system with  $m + 1$  particles (with  $j$  being the position of the extra particle). Subsequently this new system scatters off the target giving rise to the first term in the above equation, while the second (negative sign) term there corresponds to the possibility that no extra particle was created.

The physical content of this hierarchy will be further discussed on its continuum version, which reads (cf. Eq. (2.9))

---

<sup>8</sup> Of course, some of these  $m$  particles can have identical positions.

$$\frac{\partial \langle s_{x_1} \dots s_{x_m} \rangle}{\partial Y} = \int_z f_z(\{m\}) \langle s_{x_1} \dots s_{x_m} s_z - s_{x_1} \dots s_{x_m} \rangle, \quad (3.17)$$

in simplified notations where the coordinates are shown as lower indices and the  $Y$ –dependence of the expectation values is not indicated. The general structure of these equations is interesting, as it may shed light on the corresponding structure in QCD. It is especially instructive to compare these equations to the Balitsky–JIMWLK equations [12–16] and also to the more complete ‘Pomeron loop’ equations recently proposed in QCD at large  $N_c$  [2, 20, 21].

Recall at this point that the Balitsky hierarchy in QCD has been obtained by performing *different* evolutions in the projectile and the target: the projectile has been assumed to be dilute and evolve according to the dipole picture<sup>9</sup>, whereas the target was taken to be dense and evolve according to JIMWLK equation. Under these assumptions, the Balitsky equations are *formally* boost invariant, but the whole scheme is clearly incomplete and unsatisfactory, since an evolving projectile eventually becomes dense and, vice versa, even a target which looks dense on some resolution scale (at relatively low transverse momenta) has necessarily a dilute tail at high transverse momenta, and this tail is the driving force for its evolution [1].

This problem is overcome, by construction, within the toy model, where the target and the projectile are symmetrically treated, and it is interesting to see how this is reflected in the structure of the evolution equations. The first equation in the hierarchy (3.17), that is,

$$\frac{\partial \langle s_x \rangle}{\partial Y} = \int_z \frac{\tau_{xz}}{\tau} \langle s_x s_z - s_x \rangle, \quad (3.18)$$

is formally similar to the corresponding Balitsky equation, from which it differs only by the replacement of the ‘dipole kernel’ (the rate for dipole splitting in QCD) by the reduced scattering amplitude  $\tau_{xz}/\tau$ , which plays the role of the elementary splitting rate (corresponding to a parent particle in isolation) within the toy model. Note that the splitting is more constrained in the toy model than in QCD, for the reasons explained in Sect. 2: one of daughter ‘dipoles’  $x$  and  $z$  which appear in the r.h.s. of Eq. (3.18) is bound to have the same ‘size’  $x$  as its parent ‘dipole’ in the l.h.s.

It seems therefore natural to identify the elementary splitting  $x \rightarrow xz$  with rate  $\tau_{xz}/\tau$  in the toy model to the dipole splitting in QCD. With this identification, the differences between the toy–model hierarchy (3.17) and the Balitsky equations become visible in the higher equations in the hierarchy, starting with the second one:

$$\frac{\partial \langle s_x s_y \rangle}{\partial Y} = \int_z \frac{\tau_{xz} + \tau_{zy} - \tau_{xz}\tau_{zy}}{\tau} \langle s_x s_y s_z - s_x s_y \rangle. \quad (3.19)$$

The respective Balitsky equation would involve only the two positive terms,  $\tau_{xz}$  and  $\tau_{zy}$ , in the numerator in the kernel, which describe the independent splittings of the particle at  $x$  and at  $y$ , respectively. The additional, negative, term  $-\tau_{xz}\tau_{zy}$  corresponds to ‘saturation effects’ in the evolution of the projectile, namely to the fact that the two splittings are not truly independent.

---

<sup>9</sup> We here restrict ourselves to the large– $N_c$  version of the Balitsky hierarchy, as appropriate for comparison with the toy model.

This term is formally suppressed by a power of  $\tau$  with respect to the previous ones, but as we shall shortly argue it cannot be neglected, since it plays an essential role in the evolution.

This discussion can be easily generalized to the higher equations in the hierarchy: the toy–model analog of the Balitsky equations can be obtained from the general equations (3.17) by replacing the kernel  $f_z(\{m\})$  there by its linearized version (cf. Eqs. (2.10) and (3.11))

$$f_z(\{m\}) \longrightarrow \sum_{i=1}^m \frac{\tau(x_i|z)}{\tau}, \quad (3.20)$$

which describes the independent splitting  $x_i \rightarrow x_i z$  of any of the  $m$  particles in the projectile. Clearly, this is similar to QCD, since it is tantamount to saying that the projectile evolves according to the dilute approximation (2.10) to the master equation (2.4). Also like in QCD, it can be easily checked that the same set of equations would be obtained by evolving the target according to the toy–model version of the ‘JIMWLK’ equation, Eq. (2.15).

Thus, clearly, the toy–model hierarchy (3.17) goes beyond the Balitsky–JIMWLK equations by including saturation effects in the evolution of the projectile, or, equivalently, particle–number fluctuations in that of the target. It is therefore interesting to better understand the physical role of the additional term, so like the negative term in the kernel in Eq. (3.19). To that aim, and also to facilitate the comparison with the ‘Pomeron loop’ equations of QCD, it is convenient to rewrite the above equations in terms of the  $T$ –matrix elements (or ‘scattering amplitudes’)  $t_x \equiv 1 - s_x$ . We display here the first two equations in the ensuing hierarchy (the third such equation will be shown in the Appendix):

$$\frac{\partial \langle t_x \rangle}{\partial Y} = \int_z \frac{\tau_{xz}}{\tau} \langle t_z - t_x t_z \rangle, \quad (3.21)$$

and, respectively,

$$\frac{\partial \langle t_x t_y \rangle}{\partial Y} = \int_z \left[ \frac{\tau_{xz}}{\tau} \langle (t_z - t_x t_z) t_y \rangle + \frac{\tau_{yz}}{\tau} \langle (t_z - t_y t_z) t_x \rangle + \frac{\tau_{xz} \tau_{yz}}{\tau} \langle t_z (1 - t_x)(1 - t_y) \rangle \right]. \quad (3.22)$$

Notice that  $t_x t_y = (1 - s_x)(1 - s_y)$  is the amplitude for the *simultaneous* scattering of two particles in the projectile. At this level, it becomes straightforward to recognize the toy–model analogs of the BFKL and, respectively, BK equation: the former is obtained by neglecting the non–linear term  $\langle t_x t_z \rangle$  in the r.h.s. of Eq. (3.21), while the second corresponds to treating this term in a mean–field approximation (MFA) which assumes factorization:  $\langle t_x t_z \rangle \approx \langle t_x \rangle \langle t_z \rangle$ . However, this factorization is inconsistent with the higher equations in the hierarchy, starting with Eq. (3.22). This breakdown of the MFA is associated with the presence of ‘fluctuation terms’, like the last term  $\propto \tau_{xz} \tau_{zy}$  in the r.h.s. of Eq. (3.22), which are precisely the additional terms with respect to the (toy–model) Balitsky equations. Such terms are important, since they generate the correlations in the dilute regime, as we explain now:

Consider indeed the regime in which the target is so dilute that the average scattering amplitude is *very weak*<sup>10</sup>:  $\langle t \rangle \lesssim \tau$ . This corresponds to the dilute tail of the target distribution at large values of  $x$ , where the (average) occupation number is  $\langle n \rangle \lesssim 1$ . (Indeed, in the dilute

---

<sup>10</sup> The relevance of this regime for the high–energy evolution will be explained in Sects. 4 and 5.

regime, one can write  $\langle t_x \rangle \approx \int_z \tau_{xz} \langle n_z \rangle$ ; see, e.g., Eq. (2.6).) In this regime, the last term in the r.h.s. of Eq. (3.22) can be approximated as  $(\tau_{xz}\tau_{yz}/\tau) \langle t_z \rangle$ , which for  $\langle t \rangle \lesssim \tau$  is comparable to, or even larger than, the BFKL-like terms in that equation, so like  $(\tau_{xz}/\tau) \langle t_z t_y \rangle$ . This shows that, in this dilute regime, the two-particle amplitude  $\langle tt \rangle$  is still very small but it gets built from the one-particle amplitude  $\langle t \rangle$ , via the last term in Eq. (3.22). To better appreciate the physical interpretation of this term, notice that in the dilute regime one can successively write

$$\frac{\partial \langle t_x t_y \rangle}{\partial Y} \Big|_{\text{fluct}} \simeq \int_z \frac{\tau_{xz}\tau_{yz}}{\tau} \langle t_z \rangle \simeq \int_z \frac{\tau_{xz}\tau_{yz}}{\tau} \int_w \tau_{zw} \langle n_w \rangle \simeq \int_z \tau_{xz}\tau_{yz} \frac{\partial \langle n_z \rangle}{\partial Y}, \quad (3.23)$$

where we have also used the appropriate limit of Eq. (3.12). According to this equation, the change in the two-particle amplitude  $\langle t_x t_y \rangle$  in one step of the evolution can be interpreted as the following evolution in the target: first, a new particle is created at  $z$ , via the splitting process  $w \rightarrow wz$ , with any  $w$ ; then, the new target particle at  $z$  scatters simultaneously with the two projectile particles at  $x$  and  $y$ .

We see that the two-particle correlation  $\langle t_x t_y \rangle - \langle t_x \rangle \langle t_y \rangle$  gets built from ‘target fluctuations’ (i.e., splitting processes leading to a change in the particle number in the target distribution), via *multiple scattering*. This mechanism is quite similar to that identified in the context of QCD in Ref. [2], and which has inspired an extension of the Balitsky–JIMWLK hierarchy known as the ‘Pomeron loop’ hierarchy [2, 20, 21]. The general structure of this ‘Pomeron loop’ hierarchy is indeed similar to that for the scattering amplitudes in the toy model (cf. Eqs. (3.21)–(3.22)), in the sense of including BFKL terms, non-linear terms responsible for unitarization, and fluctuation terms which generate correlations in the dilute regime. However, some subtle differences persist, which can be partly attributed to real structural differences between the dynamics in QCD and that in the toy model, and partly to the different ways how perturbation theory is organized in the two cases. It turns out that it is instructive to understand these differences in more detail, as they shed new light on the QCD equations themselves. This will be discussed at length in the Appendix, where we shall see the two sets of equations are essentially equivalent at low density, but they potentially differ from each other in their respective extensions towards the high-density regime. In that sense, the lessons drawn from the toy model may suggest improvements of the ‘Pomeron loop’ equations in QCD.

## 4 Analytic results: From BFKL growth to diffusive scaling

In this section we shall present an analytic study of the evolution described by the toy model which mimics the corresponding analysis of the high energy evolution in QCD, as standard by now in the literature (see especially Refs. [1, 2, 30, 31, 33, 36]). We shall thus successively address the linear approximation (which corresponds to the BFKL equation [7] in QCD), the mean field approximation (the toy-model analog of the BK equation [13]), and, finally, the effects of particle-number fluctuations, that we shall describe by analogy<sup>11</sup> with the reaction–diffusion problem in statistical physics (so like in Ref. [1] for QCD).

---

<sup>11</sup> The pertinence of this analogy for the particle model at hand will be confirmed by the numerical analysis of this model in Sect. 5.

For the purposes of this analysis, we need to be more specific about the form of the elementary particle-particle scattering amplitude  $\tau(x|z)$ . Inspired by the analogy with QCD, in which this quantity corresponds to the amplitude for dipole-dipole scattering, we shall choose

$$\tau(x|z) = \tau \exp(-|x - z|). \quad (4.1)$$

The QCD-origin of this formula can be recognized as follows: after translating to QCD notations, that is,  $x \equiv \ln(r_0^2/r^2)$  with  $r$  the current dipole size and  $r_0$  an arbitrary scale of reference, Eq. (4.1) becomes equivalent to  $\tau(r_1|r_2) = \tau r_<^2/r_>^2$ , where  $r_< = \min(r_1, r_2)$  and  $r_> = \max(r_1, r_2)$ . With the further identification  $\tau = \alpha_s^2$ , the latter is a good approximation to the amplitude for the central scattering between two elementary dipoles in QCD. By ‘central’ we mean, as usual, a collision at zero relative impact parameter. It is also understood that the amplitude is averaged over the orientations of the two-dimensional vectors  $\mathbf{r}_1$  and  $\mathbf{r}_2$ .

#### 4.1 BFKL evolution in the toy model

We shall focus on the equations obeyed by the dipole scattering amplitudes and start with the linearized version of Eq. (3.21), which plays the role of BFKL equation [7] within the toy model. With the specific form of  $\tau_{xz}$  given above, this equation reads

$$\frac{\partial t_x}{\partial Y} = \int dz \exp(-|x - z|) t_z \quad (4.2)$$

(averages are implicitly assumed). Defining the Mellin transform with respect to  $\exp(-x)$

$$\tilde{t}(\gamma, Y) = \int_{-\infty}^{\infty} dx \exp(\gamma x) t(x, Y), \quad (4.3)$$

one finds that  $\tilde{t}(\gamma, Y) = \tilde{t}(\gamma, Y=0) \exp[\chi(\gamma) Y]$  where the ‘characteristic function’  $\chi(\gamma)$  is the Mellin transform of the kernel in Eq. (4.2) and reads

$$\chi(\gamma) = \frac{1}{1 - \gamma} + \frac{1}{1 + \gamma}. \quad (4.4)$$

Then the general solution to Eq. (4.2) is obtained as

$$t(x, Y) = \int_{\mathcal{C}} \frac{d\gamma}{2\pi i} \tilde{t}(\gamma, 0) \exp[\chi(\gamma)Y - \gamma x], \quad (4.5)$$

where the integration contour  $\mathcal{C}$  is parallel to the imaginary axis and with its real part being such that  $|\text{Re}(\gamma)| < 1$ . From Eq. (4.3) it is clear that  $\tilde{t}(\gamma, 0)$  is the Mellin transform of the scattering amplitude at  $Y = 0$ . For definiteness, we shall assume that the target is initially composed a single dipole of size  $r_0 = \exp(-x_0/2)$ , in which case we have  $\tilde{t}(\gamma, 0) = \tau \chi(\gamma) \exp(\gamma x_0)$ .

Let us now analyze some special limits of Eq. (4.5), to which we shall refer by using a QCD-inspired terminology:

(i) *The Pomeron intercept* : Consider the high-energy limit  $Y \rightarrow \infty$  at fixed  $x$  (which is the limit used in QCD to define the ‘Pomeron intercept’). In the kinematical plane  $(Y, x)$ , this

corresponds to the evolution along a (nearly) vertical axis. In this limit, the integral is dominated by the region around the point  $\gamma_{\mathbb{P}}$  that satisfies  $\chi'(\gamma_{\mathbb{P}}) = 0$ . One easily finds  $\gamma_{\mathbb{P}} = 0$  and  $\chi(\gamma_{\mathbb{P}}) = 2$ , and by also performing the Gaussian integration around this saddle point one obtains

$$t(x, Y) = \frac{\tau}{\sqrt{2\pi Y}} \exp \left[ 2Y - \frac{(x - x_0)^2}{8Y} \right]. \quad (4.6)$$

The  $Y$ -dependence of the amplitude is similar to the QCD one, as in both cases it increases exponentially in  $Y$ . (Recall that in QCD the dominant  $Y$ -dependence in this limit is  $\sim \exp(\omega_{\mathbb{P}} Y)$ , with  $\omega_{\mathbb{P}} = 4 \ln 2$ .) However the analogy is not complete, since the toy-model amplitude as given above is independent<sup>12</sup> of the projectile dipole size  $r$ . By contrast, the respective amplitude in QCD is proportional to  $r$ , which is however a relatively ‘weak’ dependence when compared to the corresponding result at fixed order perturbation theory, namely  $t(r) \sim r^2$  (‘color transparency’). Note also the Gaussian dependence of Eq. (4.6) upon  $x - x_0$ , which describes diffusion with a diffusive radius  $\propto Y^{1/2}$ . This is again similar to the well-known BFKL diffusion in the logarithmic variable  $\ln(1/r^2)$ .

(ii) *Double logarithmic approximation (DLA)* : This is the evolution along a direction in the plane  $(Y, x)$  which is such that the difference  $x - x_0$  between the dipole sizes increases faster than the rapidity  $Y$ . When  $x - x_0 \gg Y$ , the integral is dominated by a value of  $\gamma$  which is close to 1. The saddle point occurs at  $\gamma_{\text{DLA}} = 1 - [Y/(x - x_0)]^{1/2}$  and we are lead to

$$t(x, Y) = \frac{\tau}{2\sqrt{\pi}} [(x - x_0)Y]^{-1/4} \exp \left[ -(x - x_0) + \sqrt{4(x - x_0)Y} \right]. \quad (4.7)$$

This is exactly the same as the corresponding QCD result, which should not come as a surprise: in the ‘double logarithmic limit’ of QCD, one of the daughter dipoles has a size equal to the parent one, a feature which is a built-in in the one-dimensional model under consideration. In particular, the above result shows ‘color transparency’, that is,  $t(x) \propto \exp[-(x - x_0)]$ , in full analogy with the QCD behaviour  $t(r) \sim r^2$  at very small values of  $r$ .

## 4.2 Unitarity corrections in the mean field approximation

As explicit in the previous analysis, the high-energy evolution described by Eq. (4.2) leads to a scattering amplitude which rises rapidly with  $Y$  (cf. Eq. (4.6)), and thus eventually violates the unitarity bound  $t \leq 1$ . So, to study the high-energy behaviour, one needs to include the non-linear terms responsible for unitarity corrections. We shall first do so within the *mean field approximation*  $\langle t_x t_y \rangle \approx \langle t_x \rangle \langle t_y \rangle$ , in which Eq. (3.21) reduces to a closed, non-linear equation (the expectation values are again implicit)

$$\frac{\partial t_x}{\partial Y} = \int dz \exp(-|x - z|) (t_z - t_x t_z) \quad (4.8)$$

---

<sup>12</sup> In the QCD terminology, the high-energy solution (4.6) exhibits an ‘anomalous dimension’  $1 - \gamma_{\mathbb{P}} = 1$ , which is the maximal possible value; for comparison, this value is  $1/2$  for the corresponding solution to the BFKL equation.

which is the toy model analog of the BK equation in QCD [12, 13]. This analogy is not only formal, but it covers several essential aspects: (a) Like the BK equation, Eq. (4.8) is consistent with unitarity and, moreover, its solution approaches the unitarity bound at large  $Y$  (as obvious from the fact that  $t = 1$  is a fixed point). (b) In the weak scattering limit  $t \ll 1$ , Eq. (4.8) reduces, as we have seen, to a linear equation which describes an exponential increase with  $Y$  and diffusion in  $x$ . Together, these properties imply Eq. (4.8) is in the universality class of the FKPP equation [4], so like the BK equation itself [33], which in turn implies that the evolution towards saturation is driven by the linear dynamics in the dilute regime — the precise form of the non-linear terms is unimportant so long as they provide saturation. It is then easy to adapt the analysis of the BK equation in Refs. [17, 31, 33] to Eq. (4.8), with the following results:

For sufficiently large values of  $Y$  (in order to loose memory of the initial condition and reach a universal behaviour), the solution  $t(x, Y)$  is a *traveling wave*, that is, a front which interpolates between  $t = 1$  at large negative values of  $x$  and  $t \rightarrow 0$  at large positive values and which propagates towards larger values of  $x$  when increasing  $Y$ . The position  $x_s(Y)$  of this front defines the *saturation line*, that is, the direction of evolution in the plane  $(Y, x)$  along which the scattering amplitude is constant and of  $\mathcal{O}(1)$ . As mentioned before, the location of this line can be inferred from the solution to the linearized ('BFKL') equation (4.2). We thus return to this solution, Eq. (4.5), and consider a third direction of evolution in the  $(Y, x)$ -plane, that corresponding to the saturation line:

(iii) *The saturation line* : When increasing the rapidity along this line, the position  $x$  (i.e., the inverse dipole size) should be correspondingly increased in order for the amplitude to remain constant. For  $Y$  large enough, one can use the saddle point approximation in Eq. (4.5). The saddle point condition

$$\chi'(\gamma_s)Y - x_s = 0, \quad (4.9)$$

together with the condition that the exponent vanishes (in order for the amplitude to be roughly constant) along the saturation line

$$\chi(\gamma_s)Y - \gamma_s x_s = 0, \quad (4.10)$$

uniquely determine the value of the saturation saddle point  $\gamma_s$  and the line  $x_s(Y)$  (the latter up to an additive constant), which in this approximation is simply a straight line:  $x_s(Y) \approx \lambda_s Y$ . Namely, one finds

$$\chi'(\gamma_s) = \frac{\chi(\gamma_s)}{\gamma_s} \Rightarrow \gamma_s = \frac{1}{\sqrt{3}}, \quad \text{and} \quad \lambda_s = \frac{\chi(\gamma_s)}{\gamma_s} = 3\sqrt{3}. \quad (4.11)$$

It is in fact possible to improve our estimate for  $\lambda_s$  by more properly taking into account the non-linear effects. (Within the context of the linear equation, this requires introducing an absorptive boundary parallel to the saturation line; see Ref. [31] for details.) One thus finds

$$\lambda_s \equiv \frac{dx_s(Y)}{dY} \approx \frac{\chi(\gamma_s)}{\gamma_s} - \frac{3}{2\gamma_s Y} = 3\sqrt{3} - \frac{3\sqrt{3}}{2Y}, \quad (4.12)$$

in agreement with results from the FKPP equation [4]. To the same accuracy, the amplitude in

the vicinity of the saturation line can be obtained via an expansion around the saturation saddle point, which yields

$$t(x, Y) = c_1 \tau(x - x_s + c_2) \exp \left[ -\gamma_s(x - x_s) - \frac{(x - x_s)^2}{2\chi''(\gamma_s)Y} \right]. \quad (4.13)$$

This is strictly valid for  $1 \ll x - x_s \ll 2\chi''(\gamma_s)Y$ , which is a parametrically large window at large  $Y$ . In Eq. (4.13),  $c_1$  and  $c_2$  are unknown constants of order  $\mathcal{O}(1)$ ,  $\chi''(\gamma_s) = 27$ , and the linear factor  $x - x_s$  arises from the absorptive boundary.

We notice that in the region  $x - x_s \ll \sqrt{2\chi''(\gamma_s)Y}$ , where the diffusion term in the exponent in Eq. (4.13) can be neglected, the amplitude exhibits *geometric scaling*, i.e. it depends on  $x$  and  $Y$  only through the combined variable  $x - x_s(Y)$ . This is what one means by a ‘traveling wave’ [33] : a front which when increasing  $Y$  gets simply translated towards larger values of  $x$ , without being distorted.

It is furthermore instructive to translate the above picture to the average particle number in the target,  $n(x, Y)$ . In the tail of the front at  $x \gg x_s(Y)$ , where  $t \ll 1$ , we have  $t(x, Y) \approx \int dz \tau(x|z)n(z, Y)$ , where the  $z$ -integration is peaked at  $z = x$ . Thus, a ‘small’ (large- $x$ ) incoming ‘dipole’ scatters off target ‘dipoles’ with a similar ‘size’ ( $z \sim x$ ), and the weakness of the interaction corresponds to the fact that the target looks *dilute* on this resolution scale:  $n(x, Y) \ll 1/\tau$ . When increasing  $Y$  in this dilute regime,  $n$  rises very fast, exponentially in  $Y$ , so like  $t$ . Around the front position ( $x \sim x_s(Y)$ ), one has  $t \sim \mathcal{O}(1)$  and thus  $n \sim \mathcal{O}(1/\tau)$ : on this resolution scale, the target is *dense*. Finally, behind the front, where  $t$  saturates at 1, the occupation number does *not* saturate, rather it keeps growing with  $Y$ , albeit only slowly (cf. Eq. (3.5)):  $n(x, Y) \simeq (Y - Y_c)/\tau$ , where  $Y_c \sim \ln(1/\tau)$  is the ‘critical’ rapidity for reaching saturation in the deposit rate at  $x$ :  $f(x) = 1/\tau$  for  $Y > Y_c$ . The precise value of  $Y_c$  depends upon  $x$  and the initial conditions at  $Y = 0$ .

### 4.3 Particle number fluctuations

As discussed in Sect. 3.2, the evolution equations involve fluctuation terms, like the last term in Eq. (3.22), which reflect the discreteness of the particle number and are inconsistent with the mean field approximation underlying Eq. (4.8). Since the occupation numbers are large at saturation,  $n \sim 1/\tau \gg 1$ , one may still hope that the effects of such fluctuations are relatively small and can be treated in perturbation theory around the mean-field results. However, this expectation turns out to be naive, as only recently understood in the context of QCD [1, 2, 19, 50]. The high-energy evolution is in fact dramatically sensitive to fluctuations, and the physical reason for that is implicit in the previous discussion: the evolution is driven by the BFKL growth and diffusion in the *dilute tail* of the front, where the occupation numbers are small (of order one) and thus the effects of particle-number fluctuations are important indeed.

The previous analysis of the linear and the mean-field approximations suggests that the model under consideration falls in the universality class of the ‘reaction–diffusion’ process [4, 51] (cf. the Introduction), and this conclusion will be further supported by the numerical analysis in the next section. It is then possible — like in the corresponding studies in QCD [1, 2] — to rely on the correspondence with statistical physics in order to characterize the *universal* aspects of the dynamics in the presence of fluctuations. These aspects are mostly *qualitative* and refer

to the ‘late–time’ (here, large  $Y$ ) behaviour at ‘weak coupling’ (here,  $\tau \ll 1$ ). In fact, the *semi-quantitative* results which are known to be universal are valid only for values of  $\tau$  which are too small to be relevant for the analogy with QCD (recall that  $\tau = \alpha_s^2$ ). Yet, most of the qualitative features that we shall enumerate below will be later recognized on the numerical results in Sect. 5.

- (i) For a given initial condition at  $Y = 0$ , the stochastic evolution up to  $Y$  generates a *statistical ensemble of fronts* (rather than a single front for the deterministic dynamics in the MFA), with the different fronts in the ensemble differing by their respective front positions. Hence,  $x_s(Y)$  becomes now a *random variable*.
- (ii) To a very good approximation, the distribution of  $x_s$  at  $Y$  is a Gaussian, with an expectation value  $\langle x_s \rangle$  and a dispersion  $\sigma^2(Y) = \langle x_s^2 \rangle - \langle x_s \rangle^2$  which rise both linearly with  $Y$ :  $\langle x_s \rangle = \lambda_s Y$  and  $\sigma^2(Y) = D_f Y$ . The limitations of this Gaussian approximation have been analytically studied in Refs. [6,37] in the limit of high occupancy (or weak coupling), which amounts to letting  $\tau \rightarrow 0$  within the toy model.
- (iii) The (asymptotic) value of the *average velocity*  $\lambda_s$  is significantly smaller than its mean-field prediction in Eq. (4.11). The respective deviation is analytically known in the formal weak-coupling limit [5], with a result which when adapted to the present toy model reads

$$\lambda_s \simeq \frac{\chi(\gamma_s)}{\gamma_s} - \frac{\pi^2 \gamma_s \chi''(\gamma_s)}{2 \ln^2 \tau} = 3\sqrt{3} - \frac{9\sqrt{3} \pi^2}{2 \ln^2 \tau}, \quad (4.14)$$

valid when  $\ln^2 \tau \gg 1$ . In the same limit, the *front diffusion coefficient*  $D_f$  is known to behave like  $D_f \sim 1/\ln^3(1/\tau)$  [6], and thus to vanish, at it should, when  $\tau \rightarrow 0$ . Notice, however, the very slow, *logarithmic* in  $\tau$ , convergence of these results to their respective mean-field limits, which reflects the strong sensitivity of the evolution to fluctuations.

- (iv) When increasing  $Y$ , the asymptotic value of  $\lambda_s$  is rapidly reached (*exponentially* in  $Y$ ), as opposed to the rather slow convergence predicted by the mean-field result (4.12).
- (v) The individual fronts in the ensemble exhibit *geometric scaling*, but only over a *compact* region: that is, for each front, there is only a finite distance  $x - x_s \leq \Delta x_g$ , with  $\Delta x_g \simeq (1/\gamma_s) \ln(1/\tau)$ , ahead of the front where the amplitude scales like  $t(x) \propto e^{-\gamma_s(x-x_s)}$ , with  $\gamma_s = 1/\sqrt{3}$ . This should be contrasted to the mean-field amplitude in Eq. (4.13), for which the scaling window  $x - x_s \propto \sqrt{Y}$  is ever increasing with  $Y$ , and hence it can become arbitrarily large.
- (vi) The width  $\Delta x_g$  of the scaling window in the presence of fluctuations is precisely the distance over which the amplitude fails from its value  $t \simeq 1$  at saturation to a value of  $\mathcal{O}(\tau)$ , which is the value corresponding to an occupation number  $n(x)$  of  $\mathcal{O}(1)$ . This is not an accident: in an actual event, the occupation number per site is *discrete*,  $n(x) = 0, 1, 2, \dots$ , so it cannot fall down to a non-zero value which is smaller than one. Hence, a front in  $n(x)$  has naturally an *end point*, which is the rightmost occupied bin, and where the occupation number is of  $\mathcal{O}(1)$ . Now, the corresponding front for  $t(x)$  is not truly compact, because of the non-locality in the elementary scattering amplitude (recall that  $t(x) \approx \int dz \tau(x|z)n(z)$  in the dilute regime). However, the latter decays very fast at large distances, cf. Eq. (4.1), so for  $x - x_s \gg \Delta x_g$  the front  $t(x)$  develops an exponential tail of the ‘color transparency’ type:  $t(x) \propto e^{-x}$ .
- (vii) Physical observables, like the *average* dipole amplitude  $\langle t(x) \rangle_Y$ , are obtained by averaging

over the ensemble. In this averaging, the geometric scaling property of the individual fronts is washed out by the dispersion in the positions of the fronts [1, 19], and is eventually replaced, at sufficiently large  $Y$ , by a new type of scaling [1, 2], known as *diffusive scaling* [36]. Specifically,  $\langle t(x) \rangle_Y$  is estimated as

$$\langle t(x) \rangle_Y \simeq \frac{1}{2} \operatorname{Erfc} \left[ \frac{x - \langle x_s \rangle}{\sqrt{2D_f Y}} \right], \quad (4.15)$$

where  $\operatorname{Erfc}(x)$  is the complimentary error function:

$$\operatorname{Erfc}(x) \equiv \frac{2}{\sqrt{\pi}} \int_x^\infty dt e^{-t^2} = \begin{cases} 2 - \frac{\exp(-x^2)}{\sqrt{\pi} |x|} & \text{for } x \ll -1 \\ 1 & \text{for } |x| \ll 1 \\ \frac{\exp(-x^2)}{\sqrt{\pi} x} & \text{for } x \gg 1. \end{cases} \quad (4.16)$$

The diffusive scaling approximation, Eq. (4.15), holds when  $D_f Y \gg 1$  and in a wide region around the (average) saturation line  $\langle x_s \rangle_Y$ , such that  $|x - \langle x_s \rangle| \ll \gamma_s D_f Y$ . It also smoothly interpolates towards the black disk limit  $\langle t(x) \rangle = 1$  as  $x \rightarrow -\infty$ . For even larger distances  $x - \langle x_s \rangle \gtrsim \gamma_s D_f Y$ , one recovers the color-transparency behaviour,  $\langle t(x) \rangle \propto \exp[-(x - \langle x_s \rangle)]$ , with a prefactor which is sensitive to fluctuations (see Refs. [2, 36] for details).

## 5 Some numerical results

As mentioned in the Introduction, our present numerical investigation of the one-dimensional model is only exploratory, with the purpose of illustrating some of the analytic results and qualitative features anticipated in the previous section and, especially, verifying that the present model lies indeed in the universality class of the reaction-diffusion process. In this section, we shall briefly present our numerical technique (a Monte-Carlo simulation) and then expose the first results obtained in this way. Further verifications and more detailed results are deferred to a subsequent publication.

We would like to simulate the particle evolution described by the master equation (2.4) along with the deposit rate in Eq. (2.9). To that aim, we need to specify the one-dimensional lattice (that is, the extremal values,  $x_{\min}$  and  $x_{\max}$ , for  $x$ , and the lattice spacing  $\Delta$ ) together with the initial conditions at  $Y = 0$  and the value of the parameter  $\tau$  which enters the elementary scattering amplitude (4.1). In practice, we shall use a lattice of 1152 size bins between  $x_{\min} = -16$  and  $x_{\max} = 128$  (hence,  $\Delta = 0.125$ ). Also, we choose  $\tau = 0.01$ , which via the identification  $\tau \equiv \alpha_s^2$  corresponds to a value  $\alpha_s = 0.1$  for the coupling constant in QCD.

We are merely interested in the universal aspects of the evolution at large values of  $Y$ , which we expect to be largely insensitive to the precise form of the initial conditions. For definiteness, we choose the particle occupation number at  $Y = 0$  to be a step function:  $n(x, Y = 0) = N_0 \theta(-x)$ , with  $N_0 = 2$ . For this distribution, we can compute the initial value of the deposit rate  $f_i$  according to Eqs. (2.9) and (4.1).

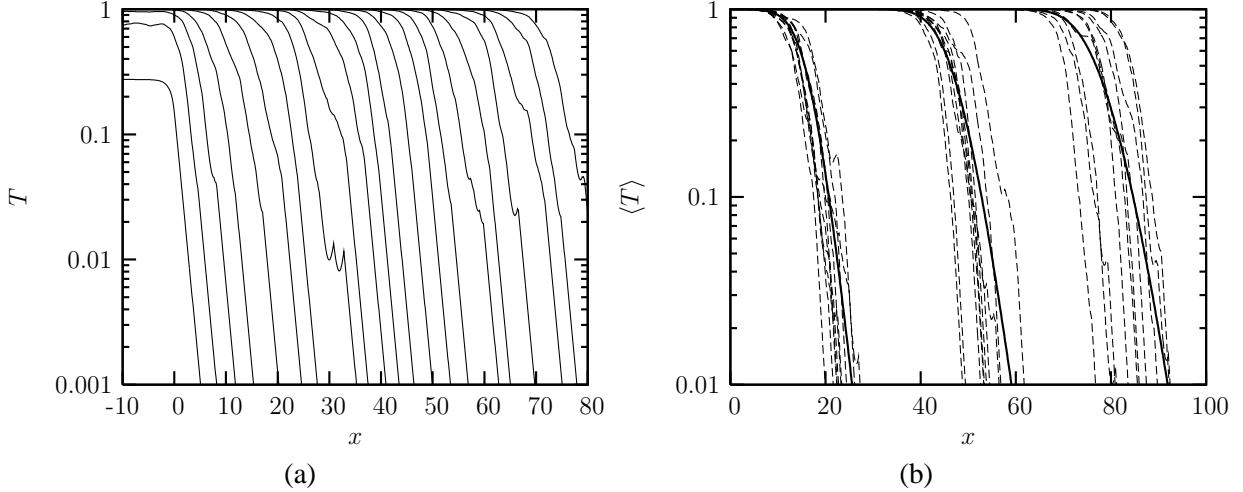


Fig. 1. Event-by-event evolution of the scattering amplitude: (a) Rapidity evolution of the scattering amplitude for a single event. (b) Amplitude for 10 events (dashed lines) and average amplitude (solid line) for  $Y = 5, 12.5, \text{ and } 20$ .

To evolve the particle system, we have to simulate particle creation according to the deposit rate  $f_i$ . One physical step in this evolution, which consists in the emission of an additional particle, involves three steps in the actual algorithm:

- (1) we first randomly select the rapidity  $\delta Y$  at which the emission occurs. This is done by generating an exponentially decreasing distribution in ‘time’ ( $Y$ ) in which the relaxation time is fixed as the inverse of the total emission rate  $\sum_i f_i$ ;
- (2) the site  $j$  at which the new particle is created is fixed by randomly selecting a site according to a probability law specified by the deposit rate (that is, to each site  $x_i$ , we attribute the weight function  $f_i$ );
- (3) the particle number is increased by one at the selected site  $j$  and the deposit rates  $f_i$  are updated for all the sites. To speed up this last step, it is useful to notice that, the only change in going from  $f_i(Y)$  to  $f_i(Y + \delta Y)$  refers to the replacement of  $n_j$  by  $n_j + 1$ . This observation together with Eq. (2.9) immediately imply

$$f_i(Y + \delta Y) = \frac{\Delta}{\tau}(1 - \sigma_{ij}) + \sigma_{ij}f_i(Y). \quad (5.17)$$

Those steps are repeated up to a maximal rapidity  $Y_{\max}$ , that we have chosen as  $Y_{\max} = 20$ . To study the stochastic aspects of the evolution, we have generated  $N_{\text{ev}} = 10^5$  distinct events.

To begin with, let us consider the rapidity evolution of a single event (see the left plot in Fig. 1). This demonstrates the formation of the traveling-wave pattern through two distinct mechanisms:

- particles are produced within already occupied sites. This evolution is basically governed by the mean-field dynamics, cf. Eq. (4.8), and results in the formation of a traveling front with the critical parameters discussed in the previous section; the (average) velocity of this front is however influenced by the fluctuations to be discussed below (cf. Eq. (4.14)).
- from time to time, a rare fluctuation appears far ahead the tip of the front, in the region that was previously unoccupied. (Such fluctuations are rare since their probability is exponen-

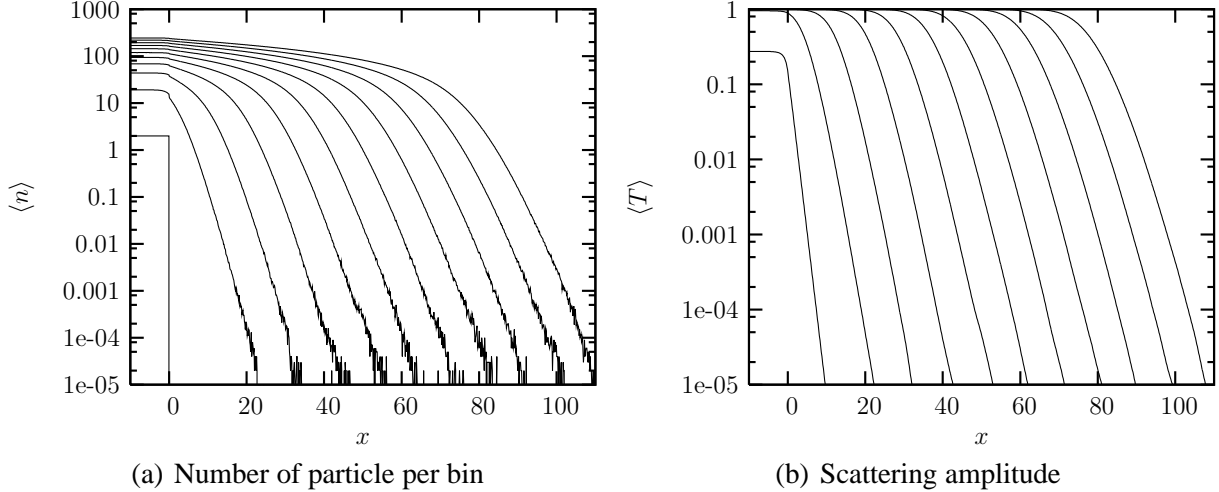


Fig. 2. Evolution of the average quantities (particle number and scattering amplitude) obtained after  $10^5$  events. Results are displayed as a function of  $x$  for, from left to right,  $Y = 0, 2, 4, \dots, 20$ .

tially decreasing with the distance to the already occupied bins, cf. Eq. (4.1).) The subsequent evolution is then a competition between the local, BFKL-like, growth of that particular fluctuation and the growth and progression of the mean-field-like wavefront. When considering a set of events, such fluctuations lead to an increasing *dispersion* in the position of the fronts (see right plot of Fig. 1), to which we shall shortly return.

By averaging over a huge number of events ( $N_{\text{ev}} = 10^5$ ), we obtain the averaged distributions shown in Fig. 2, for the average number of particles per lattice site and for the average scattering amplitude. In the left plot, we observe large fluctuations in the average number of particle per site when  $\langle n \rangle \approx 10^{-5} = 1/N_{\text{ev}}$ . Those correspond to rare fluctuations (only a few events have nonzero occupation number in the respective bins) in the dilute tail of the front. It is also interesting to notice that the fluctuations start to be visible around  $\langle n \rangle = 1/\sqrt{N_{\text{ev}}} \approx 0.003$ , as expected for particle-number fluctuations. One can also check that, within the dense regime, the number of particles per bin increases linearly as expected from Eq. (3.5).

Concerning the average amplitude, the fact that this remains smooth even in the dilute tail of the front is just because this quantity is obtained by a convolution of  $\langle n \rangle$  with the elementary interaction  $\tau_{ij}$  (recall that  $\langle t_i \rangle \approx \sum_j \tau_{ij} \langle n_j \rangle$  in the dilute regime). Still for the average amplitude, although one can notice a traveling-wave pattern in the right plot in Fig. 2, a closer look reveals that the shape of the average front is in fact changing with  $Y$  — its slope decreases with  $Y$ . This reflects the violation of geometric scaling through fluctuations, an important physical effect that we shall now study in more detail.

To that aim, we need to first study the statistics of the position of the front ('the saturation scale  $x_s$ ') as a function of rapidity. For a given event  $t(x, Y)$ , the position of the front is determined by  $t(x = x_s(Y), Y) = t_0$ , with  $t_0$  some constant number that we have here chosen as  $t_0 = 0.1$  (but we checked that different choices do not significantly modify the results). From the discussion in Sect. 4, we expect both the average value of  $x_s(Y)$  and the associated dispersion to grow linearly with  $Y$ . For the average value, this is checked on the left plot in Fig. 3, which exhibits our numerical results for  $\partial_Y \langle x_s(Y) \rangle$ . This plot further shows that the large- $Y$  asymptotic of the velocity is attained pretty fast and, moreover, this asymptotic value is sig-

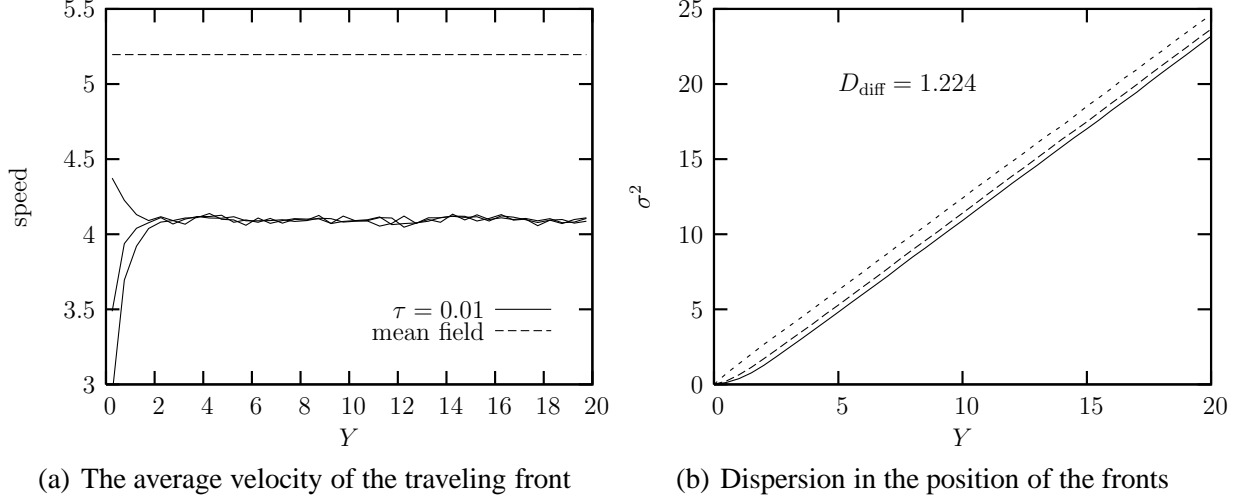


Fig. 3. The statistics of the front position (or ‘saturation scale’)  $x_s$ . Both the average position and the squared dispersion increase linearly with rapidity.

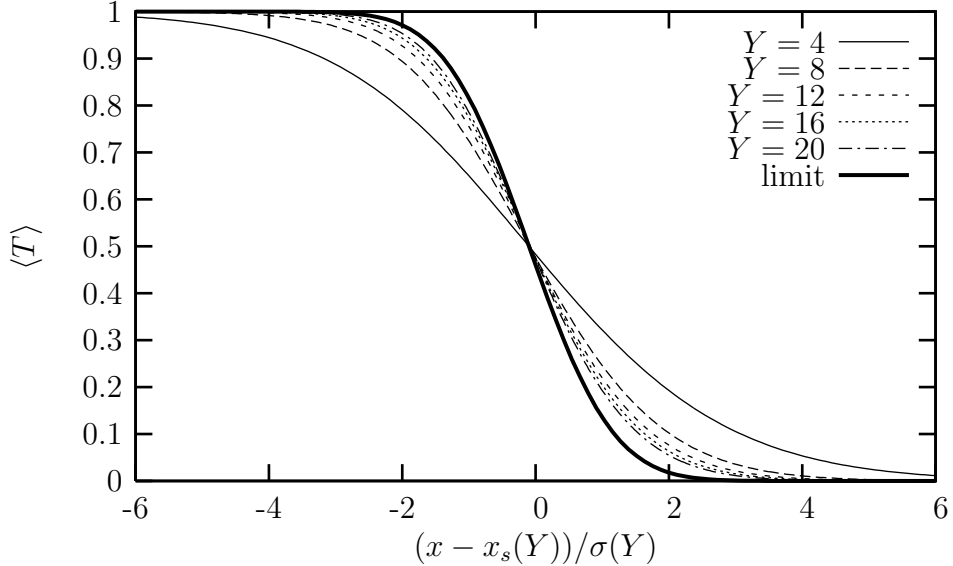


Fig. 4. The average amplitude represented as a function of the diffusive scaling variable. When rapidity increases, the asymptotic result (4.15) (indicated in the figure by ‘limit’) is indeed obtained.

nificantly smaller than the corresponding prediction of the mean-field approximation, namely  $\lambda_s = 3\sqrt{3}$  (cf. Eq. (4.11)). Next, we turn the corresponding dispersion,  $\sigma^2 = \langle x_s^2 \rangle - \langle x_s \rangle^2$ , with the results displayed in the right plot in Fig. 3. This is well fitted by a linear increase,  $\sigma^2 \simeq D_f Y$ , with a ‘front diffusion’ coefficient  $D_f = 1.224$ . Thus, the statistics of the ‘saturation scale’ follows indeed the pattern expected for a ‘reaction–diffusion’ process. We are not in a position here to also check more quantitative aspects, so like the slow approach towards the respective mean-field results with decreasing  $\tau$ , since the parameter  $\tau$  in our calculation not only has a fixed value, but this value is also too large for analytic formulæ like Eq. (4.14) to apply.

We now return to an analysis of the shape of the average amplitude (cf. the right plot in Fig. 2), with the purpose of verifying another important prediction of the ‘reaction–diffusion’

problem: the emergence of *diffusive scaling* at large  $Y$  (cf. Eq. (4.15)). To check that, we have plotted the average amplitude obtained from our numerical simulations as a function of the expected scaling variable  $(x - \langle x_s \rangle)/\sigma$ , with  $\langle x_s \rangle$  and  $\sigma^2$  taken from our previous analysis (Fig. 3) at various values of  $Y$ . As manifest on Fig. 4, the measured average amplitude converges indeed towards the expected asymptotic curve, Eq. (4.15), when increasing  $Y$ . The diffusive scaling property is thus fully satisfied by our model.

## 6 Conclusions

In this paper we have presented a (1+1)-dimensional stochastic particle model which mimics high-energy evolution and scattering in QCD at fixed impact parameter. The ‘time’ coordinate  $Y$  in this model corresponds to rapidity, while the ‘spatial’ coordinate  $x$  represents the (logarithm of the) transverse size of a dipole in QCD. The model is interesting in several respects:

- (i) The structure of the model is consistent with, and to a large extend determined by, general physical principles which are known to hold in QCD: boost-invariance, multiple scattering, and evolution via the emission of an additional particle per unit rapidity.
- (ii) Related to the above, the model exhibits a saturation mechanism which is similar to gluon saturation in QCD: The new particles created by the evolution are *coherently* emitted from the preexisting ones, with an emission rate which saturates at high density because of the multiple scattering between the additional particle and its ‘parents’.
- (iii) The model appears to be in the universality class of the reaction–diffusion process, as also expected for QCD, but unlike other related models in the literature, it does not involve explicit vertices for particle recombination. These would be redundant since saturation is anyway ensured by coherence effects in the particle emission, as explained above.
- (iv) The model exhibits all the qualitative features expected in QCD at fixed impact parameter, concerning both the mean-field aspects (a BFKL-like growth in the dilute regime, the formation of a saturation front with geometric scaling) and the effects of fluctuations (dispersion in the positions of the fronts, breakdown of geometric scaling in the statistical description, convergence towards diffusive scaling at high energy).
- (v) The model is simple enough to allow for detailed numerical investigations. Hence, it can be used as a playground to develop and test our intuition concerning the dynamics in QCD at high energy. Complex phenomena which are expected, but not yet demonstrated, in QCD (like the emergence of diffusive scaling) can be visualized in this context and their physical consequences can be explicitly analyzed.
- (vi) The structural aspects of the model are particularly interesting since they may inspire our searches for corresponding structures in QCD. In particular, the evolution equations for the scattering amplitudes in this model appear as a natural generalization (within the limits of the model, of course) of the Balitsky–JIMWLK equations in which the projectile and target are *symmetrically* treated: for each of these two systems, the equations include particle–number fluctuations and multiple scattering with both the particles internal to the system (saturation effects) and those in the other system (unitarity corrections).

In the remaining part of this concluding section we would like to elaborate a little bit more on the last point above and comparatively discuss the evolution equations in the toy model and the ‘Pomeron loop’ equations proposed in QCD at large  $N_c$  [2,20,21]. This comparison is discussed

in more detail in the Appendix from which we shall extract here the main conclusions.

By inspection of the two sets of equations — see, e.g., Eqs. (3.21), (3.22) and (A.1) for the toy model, and, respectively, Eqs. (2.7)–(2.8) in Ref. [21] for QCD —, one can notice some important differences which formally refer to the structure and physical interpretation of the respective fluctuation terms: Within the toy model, we have seen (cf. Eq. (3.23)) that these terms correspond to the multiple scattering of *only one* among the two child particles produced by a splitting in the target with two (or more) particles from the projectile. By contrast, these particular multiple-scattering effects are not at all included in the respective ‘Pomeron loop’ equations, where the fluctuation terms rather refer to the *separate* scattering of *both* child dipoles produced after a splitting in the target with two (different) dipoles in the projectile. However, as explained in the Appendix, such differences seem to be inessential (except in the very early stages of the evolution) since they amount to a reorganization of the perturbation theory in the dilute regime, which however leads to the same dominant behaviour at sufficiently high energy — namely, such that  $Y \gtrsim 1$  in the toy model and, respectively,  $\bar{\alpha}_s Y \gtrsim 1$  in QCD.

To briefly explain this reorganization, let us consider the weak-scattering regime, where the scattering amplitude for a projectile made with  $k$  particles can be estimated as (for  $Y \gtrsim 1$ )

$$\left\langle t^{(k)}(x_1, \dots, x_k) \right\rangle_Y = \int_{z_i} \tau(x_1|z_1) \cdots \tau(x_k|z_k) \left\langle n^{(k)}(z_1, \dots, z_k) \right\rangle_Y, \quad (6.1)$$

where  $\langle n^{(k)} \rangle$  is the ‘normal-ordered’  $k$ -body density of Eq. (3.6). This formula assumes that the  $k$  external particles scatter off  $k$  *different* particles in the target, and thus treats the target and the projectile on the same footing — multiple scattering is neglected for both of them. Strictly speaking, Eq. (6.1) is not the same as the  $k$ -particle scattering amplitude in fixed order perturbation theory (the latter would include additional contributions associated with the multiple scattering of individual target particles; see, e.g., Eq. (A.3) in the Appendix), but it becomes equivalent to the latter when  $Y \gtrsim 1$  since it captures the contribution which has the fastest rise with  $Y$  (the  $k$ -Pomerons piece of the complete amplitude).

In QCD at low density (and large  $N_c$ ), one can define ‘bare’ amplitudes similar to Eq. (6.1) in terms of dipoles and then deduce linear evolution equations for these quantities within the dipole picture [21]. The ‘Pomeron loop’ equations are then obtained by completing these linear equations with the non-linear terms responsible for unitarity corrections, as taken over from the Balitsky–JIMWLK equations. This procedure amounts to dressing the ‘bare’ amplitudes  $\langle t^{(k)} \rangle$  with multiple-scattering effects *on the side of the projectile*. In the toy model, on the other hand, the evolution equations obtained in Sect. 3.2 correspond to dressing  $\langle t^{(k)} \rangle$  with multiple scattering *on both the projectile, and the target, sides*.

Clearly, the last procedure is conceptually more satisfactory, as it provides a symmetric treatment of the target and the projectile in the general, strong-scattering, regime. In QCD, such a symmetric description is still lacking and its construction remains as an important open problem. But although conceptually, and also aesthetically, more appealing, it is not clear to us whether such a symmetric description would differ indeed — in terms of *physical consequences* at high energy — from that provided by the already known ‘Pomeron loop’ equations.

## Acknowledgments

G.S. is funded by the National Funds for Scientific Research (FNRS, Belgium). J.T.S.A. is partially funded by CNPq and CAPES, Brazil.

## A On the fluctuation terms in the Pomeron loop equations

In this Appendix we shall describe and clarify some structural differences between the evolution equations generated by the toy model and the Pomeron loop equations in QCD [2, 20, 21]. To that aim, it is useful to also have under ones eyes the third equation in the toy–model hierarchy, as obeyed by  $\langle t_x t_y t_z \rangle$ ; this reads:

$$\begin{aligned} \frac{\partial \langle t_x t_y t_z \rangle}{\partial Y} = & \int_w \frac{\tau_{xw}}{\tau} \langle t_w t_y t_z (1 - t_x) \rangle + \text{permutations} \\ & + \int_w \frac{\tau_{xw} \tau_{wy}}{\tau} \langle t_w t_z (1 - t_x) (1 - t_y) \rangle + \text{permutations} \\ & + \int_w \frac{\tau_{xw} \tau_{yw} \tau_{zw}}{\tau} \langle t_w (1 - t_x) (1 - t_y) (1 - t_z) \rangle. \end{aligned} \quad (\text{A.1})$$

Already a superficial comparison between the toy–model equations, cf. Eqs. (3.21)–(3.22) and (A.1), and the corresponding equations in QCD, cf. Ref. [21], reveals some important dissimilarities that we summarize here:

(A) The equation for  $\langle t^k \rangle \equiv \langle t_{x_1} \dots t_{x_k} \rangle$  within the toy model involve several types of fluctuation, with the following generic structures:  $\tau \langle t^{k-1} \rangle$ ,  $\tau^2 \langle t^{k-2} \rangle$ ,  $\dots$ ,  $\tau^{k-1} \langle t \rangle$ . These terms are all of the same order in the low density regime where  $\langle t \rangle \sim \tau$ , and hence contribute on equal footing to building up the many–body correlations. By contrast, the corresponding<sup>13</sup> ‘Pomeron loop’ equation for  $\langle T^{(k)} \rangle$  involves just one fluctuation term, with the generic structure  $\tau \langle T^{(k-1)} \rangle$  (where  $\tau \sim \mathcal{O}(\alpha_s^2)$  in QCD).

(B) As discussed in relation with Eq. (3.23), the fluctuation term in the equation for  $\langle t_x t_y \rangle$  corresponds to the double scattering of one of the daughter particles produced by a splitting in the target. A similar conclusion applies to the higher equations in the toy–model hierarchy, like Eq. (A.1): a term like  $(\tau_{xw} \tau_{wy} / \tau) \langle t_w t_z \rangle$  in the second line of Eq. (A.1) describes a process in which the two external particles at  $x$  and  $y$  scatter off the daughter particle produced at  $w$  after a splitting in the target (with the third external particles at  $z$  being just a spectator); also, a term like  $(\tau_{xw} \tau_{yw} \tau_{zw} / \tau) \langle t_w \rangle$  in the third line there corresponds to a *triple* scattering for the target particle at  $w$ , which now scatters off all the external particles.

By contrast, in the construction [2, 20, 21] of the fluctuation terms in the Pomeron loop equations in QCD, one has completely neglected the multiple scattering for the individual target dipoles. Rather, the fluctuation terms included in these equations describe the separate scattering

---

<sup>13</sup> Note that we use the upper–case notation  $T$  for the scattering amplitude of a dipole in QCD to distinguish from the respective amplitudes  $t$  in the toy model.

of *both* child dipoles produced after a splitting in the target with a pair of projectile dipoles.

The above discussion rises several questions:

- (i) Why there are no fluctuation terms in the toy–model equations corresponding to the *single* scattering of both particles  $w$  and  $z$  produced after a splitting  $w \rightarrow wz$  in the target ?
- (ii) Was it correct to neglect multiple scattering for the individual target dipoles in the corresponding equations in QCD ?
- (iii) What should be the complete structure of the fluctuation terms in QCD ?

We are not so ambitious to try and fully answer question (iii) in what follows, but we would like to clarify at least the answers to the first two questions. Specifically, we will show that the reason why the two sets of equations look so different is because they apply to *different* quantities which however have the *same dominant behaviour* at high energy (namely, for  $Y \gtrsim 1$ ).

The following considerations will be restricted to a *dilute target*, off which the individual projectile particles scatter only once. It is then preferable to express the scattering amplitudes in terms of particle densities in the target and follow the evolution of the latter. By using

$$t(x) \equiv 1 - \exp \left[ \int dz n(z) \ln \sigma(x|z) \right] \approx \int dz \tau(x|z) n(z) \quad (\text{A.2})$$

(with the last, approximate, equality valid in the dilute regime), together with the definition (3.10) of the normal–ordered pair density, one can immediately deduce

$$\langle t_x t_y \rangle \approx \int_{z,w} \tau_{xz} \tau_{yw} \langle n_z n_w \rangle = \int_{z,w} \tau_{xz} \tau_{yw} \langle n_{zw}^{(2)} \rangle + \int_z \tau_{xz} \tau_{yz} \langle n_z \rangle, \quad (\text{A.3})$$

where the contribution proportional to  $\langle n^{(2)} \rangle$  describes the scattering between the two projectile particles and two *different* target particles, while that involving  $\langle n \rangle$  describes the double scattering of a *same* target particle. We shall simultaneously consider the following quantity

$$\langle t_{xy}^{(2)} \rangle = \int_{z,w} \tau_{xz} \tau_{yw} \langle n_{zw}^{(2)} \rangle, \quad (\text{A.4})$$

which represents the toy–model analog of the 2–dipole scattering amplitude  $\langle T^{(2)} \rangle$  which enters the ‘Pomeron loop’ equations in QCD [2, 21]. As compared to Eq. (A.3), the double–scattering terms are neglected in Eq. (A.4), which therefore treats more symmetrically the target and the projectile in this weak–scattering regime (in the sense that all the particles undergo single scattering). However, it is a priori the less symmetric formula, Eq. (A.3), which yields the 2–particle scattering amplitude at fixed order in perturbation theory: indeed, both terms in the r.h.s. of Eq. (A.3) are of  $\mathcal{O}(\tau^2)$ . A similar discussion applies to the  $k$ –particle amplitudes —  $\langle t^k \rangle$  and respectively  $\langle t^{(k)} \rangle$  — with  $k \geq 3$ .

In what follow we shall use the evolution equations obeyed by the particle densities in the dilute regime to deduce the respective equations for  $\langle t^2 \rangle$  and  $\langle t^{(2)} \rangle$ . For the former, we shall recover, as expected, the linear part of the general equation (3.22), but with a more transparent interpretation for the fluctuation terms, which will also answer question (i) above. For the latter, we shall find the toy–model analog of the second equation in the ‘Pomeron loop’ hierarchy.

The low-density versions of Eqs. (3.12) and (3.13) read

$$\frac{\partial \langle n_z \rangle}{\partial Y} \approx \int_u \frac{\tau_{zu}}{\tau} \langle n_u \rangle , \quad (\text{A.5})$$

$$\frac{\partial \langle n_{zw}^{(2)} \rangle}{\partial Y} \approx \int_u \left[ \frac{\tau_{zu}}{\tau} \langle n_{uw}^{(2)} \rangle + \frac{\tau_{uw}}{\tau} \langle n_{zu}^{(2)} \rangle \right] + \frac{\tau_{zw}}{\tau} (\langle n_z \rangle + \langle n_w \rangle) . \quad (\text{A.6})$$

Notice the terms linear in  $\langle n \rangle$  in the r.h.s. of Eq. (A.6): these are *fluctuation terms* which generate a pair  $(z, w)$  of particles in the target via the splitting of a single original particle at  $z$ , or at  $w$ . These terms are very similar to those generated by the dipole picture in QCD [2].

The equation obeyed by  $\langle t_x t_y \rangle$  can now be obtained by taking a derivative w.r.t.  $Y$  in Eq. (A.3) and then using Eqs. (A.5)–(A.6). By inspection of these equations, one may expect this procedure to produce *two* types of ‘fluctuation terms’ (i.e., terms linear in  $\langle t \rangle$ ) : those generated by the BFKL evolution of the average particle density, cf. Eq. (A.5), and the ‘genuine’ fluctuation terms coming from the evolution of the pair density, cf. Eq. (A.6). The latter would correspond to the separate scattering of *both* particles  $w$  and  $z$  produced by the splitting in the target, and thus would be the toy-model analog of the fluctuation terms which appear in the Pomeron loops equations in QCD. However, from the previous discussion of Eq. (3.23), we know already that the relevant fluctuation term comes *fully* from the BFKL evolution of  $\langle n \rangle$ , cf. Eq. (A.5) ! What happens then to the fluctuation terms which are explicit in Eq. (A.6) ? As we explain now, they are in fact absorbed — via Eq. (A.3) — in the structure of the 2-particle amplitudes which enter the ‘BFKL’ terms in Eq. (3.22). Indeed, Eqs. (A.3) and (A.6) can be used to deduce

$$\begin{aligned} \int_{z,w} \tau_{xz} \tau_{yw} \frac{\partial \langle n_{zw}^{(2)} \rangle}{\partial Y} &= \int_{u,z,w} \tau_{xz} \tau_{yw} \left[ \frac{\tau_{zu}}{\tau} \langle n_u n_w \rangle + \frac{\tau_{uw}}{\tau} \langle n_z n_u \rangle \right] \\ &= \int_z \left[ \frac{\tau_{xz}}{\tau} \langle t_z t_y \rangle + \frac{\tau_{yz}}{\tau} \langle t_z t_x \rangle \right] , \end{aligned} \quad (\text{A.7})$$

where in writing the first equality we have already reabsorbed the fluctuation terms into 2-body densities like  $\langle n_u n_w \rangle$ , via Eq. (3.10). In the second line of the above equation one can recognize the BFKL terms from Eq. (3.22), as anticipated.

This answers question (i) above — the analogs of the fluctuation terms in the ‘Pomeron loop’ equations are *implicitly* included in the toy-model equations, as multiple-scattering contributions to the amplitudes which enter the BFKL terms there — but rises new questions in return : Why are these terms explicit in the QCD equations in Ref. [2, 20, 21], while they are implicit in the corresponding toy-model equations ? And why the fluctuations terms which are explicit in the toy model (those corresponding to multiple scattering off a same target particle) appear to be absent in QCD ?

The answer to these last questions, and also to the original question (ii), is that the ‘Pomeron loop’ equations are in fact written for *different* quantities, namely the ‘reduced’ scattering amplitudes  $\langle t^{(k)} \rangle$  (see Eq. (A.4)) which in this dilute regime neglect multiple scattering for both the target particles and the projectile ones. This amounts to a different reorganization of the perturbation theory in the weak-scattering regime, which however leads to the same high-energy behaviour, as previously argued in Refs. [52, 53]. (The subsequent discussion is in fact adapted

from Ref. [53].) To see this, let us consider the relative importance of the two terms in Eq. (A.3). For more clarity, assume that the target starts at  $Y = 0$  as a single particle located at  $x_0$ . Hence  $\langle n_z \rangle_0 = \delta(z - x_0)$  and  $\langle n_{zw}^{(2)} \rangle_0 = 0$ . Then, clearly, the term proportional to  $\langle n \rangle$  in Eq. (A.3) will dominate in the early stages of the evolution ( $Y \ll 1$ ), until a non-vanishing pair density gets first created via fluctuations, cf. Eq. (A.6). But once the latter becomes non-zero, its subsequent evolution is much faster — it rises as a ‘double-Pomeron’,  $\langle n^{(2)} \rangle \sim \exp(2\omega_{\mathbb{P}}Y)$  with  $\omega_{\mathbb{P}} = 2$ , while the single-density rises only as  $\langle n \rangle \sim \exp(\omega_{\mathbb{P}}Y)$  — and thus it dominates the 2-particle amplitude in Eq. (A.3) for all rapidities  $Y \gtrsim 1$ .

To summarize, in the high-energy regime where  $Y$  is relatively large,  $Y \gtrsim 1$ , but not *too* large (so that we are still in the *weak scattering regime*; this condition requires  $Y \ll \ln(1/\tau)$ ), the 2-particle scattering amplitude can be estimated simply as  $\langle t^{(2)} \rangle$ , cf. Eq. (A.4). Equivalently, this can be obtained by solving the evolution equation for  $\langle t^{(2)} \rangle$  (see below) with the initial condition  $\langle t^{(2)} \rangle_0 = 0$ . Note that this initial condition is *different* from that to be used in relation with the original equation (3.22), which follows from Eq. (A.3) and reads  $\langle t_x t_y \rangle_0 = \tau(x|x_0) \tau(y|x_0)$ .

As quite clear by inspection of Eqs. (A.4) and (A.6), the fluctuation terms in the equation for  $\langle t_{xy}^{(2)} \rangle$  come fully from the process in which the two external particles scatter off *both* child particles produced by a splitting in the target. Specifically, one finds

$$\frac{\partial \langle t_{xy}^{(2)} \rangle}{\partial Y} = \int_z \left[ \frac{\tau_{xz}}{\tau} \langle t_{zy}^{(2)} \rangle + \frac{\tau_{yz}}{\tau} \langle t_{xz}^{(2)} \rangle \right] + \frac{\partial \langle t_{xy}^{(2)} \rangle}{\partial Y} \Big|_{\text{fluct}} \quad (\text{A.8})$$

with the following expression for the fluctuation term:

$$\begin{aligned} \frac{\partial \langle t_{xy}^{(2)} \rangle}{\partial Y} \Big|_{\text{fluct}} &= \int_{z,w} \left( \tau_{xz} \tau_{yw} + \tau_{xw} \tau_{yz} \right) \frac{\tau_{wz}}{\tau} \langle n_z \rangle \\ &= \int_{z,w,u} \left( \tau_{xz} \tau_{yw} + \tau_{xw} \tau_{yz} \right) \frac{\tau_{wz}}{\tau} \tau_{zu}^{-1} \langle t_u \rangle, \end{aligned} \quad (\text{A.9})$$

where in the second line we have expressed the average particle density in the target  $\langle n_z \rangle$  in terms of the one-particle scattering amplitude  $\langle t_u \rangle$  by inverting the relation  $\langle t_u \rangle = \int_z \tau_{uz} \langle n_z \rangle$ , valid in the dilute regime. The inverse  $\tau_{xy}^{-1}$  of the elementary scattering amplitude exists indeed, since  $\tau_{xy}$  is positive-definite; in particular, for the function  $\tau_{xy}$  in Eq. (4.1), one has

$$\tau^{-1}(x|y) = \frac{1}{2\tau} (1 - \partial_x^2) \delta(x - y). \quad (\text{A.10})$$

As anticipated, Eq. (A.9) is the toy-model analog of the fluctuation term in the corresponding ‘Pomeron loop’ equation (see Eq. (2.7) in Ref. [21]). This analogy extends, of course, to the higher equations in the respective hierarchies.

We have previously noticed that, for  $Y \gtrsim 1$ , there is no important loss of accuracy if the solution  $\langle t_{xy}^{(2)} \rangle$  to Eqs. (A.8)–(A.9) with initial condition  $\langle t^{(2)} \rangle_0 = 0$  is used instead of the solution  $\langle t_x t_y \rangle$  to the more general equation (3.22) with initial condition  $\langle t_x t_y \rangle_0 = \tau(x|x_0) \tau(y|x_0)$ . By the same token we deduce that, within QCD, the solutions to the Pomeron loop equations with initial conditions  $\langle T^{(k)} \rangle_0 = 0$  for  $k \geq 2$  should provide the correct physical behaviour at high energy. This conclusion is further supported by the arguments in Ref. [52, 53].

## References

- [1] E. Iancu, A.H. Mueller and S. Munier, *Phys. Lett.* **B606** (2005) 342.
- [2] E. Iancu and D.N. Triantafyllopoulos, *Nucl. Phys.* **A756** (2005) 419.
- [3] C.W. Gardiner, *Handbook of Stochastic Methods*, (Springer series in synergetics), Springer, Berlin, 2004.
- [4] For a recent review, see W. Van Saarloos, *Phys. Rep.* **386** (2003) 29.
- [5] E. Brunet and B. Derrida, *Phys. Rev.* **E56** (1997) 2597; *Comp. Phys. Comm.* **121-122** (1999) 376; *J. Stat. Phys.* **103** (2001) 269.
- [6] E. Brunet, B. Derrida, A. H. Mueller and S. Munier, *Phys. Rev.* **E73** (2006) 056126, arXiv:cond-mat/0512021.
- [7] L.N. Lipatov, *Sov. J. Nucl. Phys.* **23** (1976) 338;  
E.A. Kuraev, L.N. Lipatov and V.S. Fadin, *Zh. Eksp. Teor. Fiz.* **72**, 3 (1977) (*Sov. Phys. JETP* **45** (1977) 199);  
Ya.Ya. Balitsky and L.N. Lipatov, *Sov. J. Nucl. Phys.* **28** (1978) 822.
- [8] A.H. Mueller, *Nucl. Phys.* **B415** (1994) 373; A.H. Mueller, B. Patel, *Nucl. Phys.* **B425** (1994).
- [9] L.V. Gribov, E.M. Levin, and M.G. Ryskin, *Phys. Rept.* **100** (1983) 1.
- [10] A.H. Mueller and J. Qiu, *Nucl. Phys.* **B268** (1986) 427.
- [11] L. McLerran and R. Venugopalan, *Phys. Rev.* **D49** (1994) 2233; *ibid.* **49** (1994) 3352; *ibid.* **50** (1994) 2225.
- [12] I. Balitsky, *Nucl. Phys.* **B463** (1996) 99; *Phys. Lett.* **B518** (2001) 235; “*High-energy QCD and Wilson lines*”, arXiv:hep-ph/0101042.
- [13] Yu.V. Kovchegov, *Phys. Rev.* **D60** (1999) 034008; *ibid.* **D61** (1999) 074018.
- [14] J. Jalilian-Marian, A. Kovner, A. Leonidov and H. Weigert, *Nucl. Phys.* **B504** (1997) 415; *Phys. Rev.* **D59** (1999) 014014; J. Jalilian-Marian, A. Kovner and H. Weigert, *Phys. Rev.* **D59** (1999) 014015; A. Kovner, J. G. Milhano and H. Weigert, *Phys. Rev.* **D62** (2000) 114005.
- [15] E. Iancu, A. Leonidov and L. McLerran, *Nucl. Phys.* **A692** (2001) 583; *Phys. Lett.* **B510** (2001) 133; E. Ferreiro, E. Iancu, A. Leonidov and L. McLerran, *Nucl. Phys.* **A703** (2002) 489.
- [16] H. Weigert, *Nucl. Phys.* **A703** (2002) 823.
- [17] E. Iancu and L. McLerran, *Phys. Lett.* **B510** (2001) 145.
- [18] L.N. Lipatov, *Nucl. Phys.* **B452** (1995) 369.
- [19] A.H. Mueller and A.I. Shoshi, *Nucl. Phys.* **B692** (2004) 175.
- [20] A.H. Mueller, A.I. Shoshi, S.M.H. Wong, *Nucl. Phys.* **B715** (2005) 440.
- [21] E. Iancu and D.N. Triantafyllopoulos, *Phys. Lett.* **B610** (2005) 253.
- [22] A. Kovner and M. Lublinsky, *Phys. Rev.* **D71** (2005) 085004.

- [23] A. Kovner and M. Lublinsky, *Phys. Rev. Lett.* **94** (2005) 181603.
- [24] J.-P. Blaizot, E. Iancu, K. Itakura, and D.N. Triantafyllopoulos, *Phys. Lett.* **B615** (2005) 221.
- [25] M. Braun, *Phys. Lett.* **B483** (2000) 115; *ibid.* **B632** (2006) 297.
- [26] Y. Hatta, E. Iancu, L. McLerran, A. Stasto, and D.N. Triantafyllopoulos, *Nucl. Phys.* **A764** (2006) 423, arXiv:hep-ph/0504182.
- [27] I. Balitsky, *Phys. Rev.* **D72** (2005) 074027, arXiv:hep-ph/0507237.
- [28] E. Iancu, G. Soyez and D.N. Triantafyllopoulos, *Nucl. Phys.* **A768** (2006) 194.
- [29] A.M. Stasto, K. Golec-Biernat and J. Kwiecinski, *Phys. Rev. Lett.* **86** (2001) 596.
- [30] E. Iancu, K. Itakura, and L. McLerran, *Nucl. Phys.* **A708** (2002) 327.
- [31] A.H. Mueller and D.N. Triantafyllopoulos, *Nucl. Phys.* **B640** (2002) 331.
- [32] D.N. Triantafyllopoulos, *Nucl. Phys.* **B648** (2003) 293.
- [33] S. Munier and R. Peschanski, *Phys. Rev. Lett.* **91** (2003) 232001; *Phys. Rev.* **D69** (2004) 034008; *ibid.* **D70** (2004) 077503.
- [34] G. Soyez, *Phys. Rev.* **D72** (2005) 016007.
- [35] R. Enberg, K. Golec-Biernat, and S. Munier, *Phys. Rev.* **D72** (2005) 074021.
- [36] Y. Hatta, E. Iancu, C. Marquet, G. Soyez, and D.N. Triantafyllopoulos, *Nucl. Phys.* **A773** (2006) 95.
- [37] C. Marquet, G. Soyez, Bo-Wen Xiao, *Phys. Lett.* **B639** (2006) 635.
- [38] E. Levin and M. Lublinsky, *Nucl. Phys.* **A763** (2005) 172.
- [39] P. Rembiesz and A.M. Stasto, *Nucl. Phys.* **B725** (2005) 251.
- [40] A. I. Shoshi and B.-W. Xiao, *Phys. Rev.* **D73** (2006) 094014.
- [41] M. Kozlov and E. Levin, *Nucl. Phys.* **A779** (2006) 142.
- [42] J.-P. Blaizot, E. Iancu, D.N. Triantafyllopoulos, hep-ph/0606253.
- [43] S. Bondarenko, L. Motyka, A.H. Mueller, A.I. Shoshi, B.-W. Xiao, *On the equivalence of Reggeon field theory in zero transverse dimensions and reaction-diffusion processes*, hep-ph/0609213.
- [44] E. Iancu and A.H. Mueller, *Nucl. Phys.* **A730** (2004) 460.
- [45] A.H. Mueller and G.P. Salam, *Nucl. Phys.* **B475** (1996) 293.
- [46] A. Kovner and M. Lublinsky, *Nucl. Phys.* **A767** (2006) 171.
- [47] A.H. Mueller, *Nucl. Phys.* **B437** (1995) 107.
- [48] A. H. Mueller, *Nucl. Phys.* **B558** (1999) 285.
- [49] E. Iancu, K. Itakura, and L. McLerran, *Nucl. Phys.* **A724** (2003) 181.
- [50] E. Iancu and A.H. Mueller, *Nucl. Phys.* **A730** (2004) 494.

- [51] For a recent review, see D. Panja, *Phys. Rep.* **393** (2004) 87 [arXiv:cond-mat/0307363].
- [52] C. Marquet, A.H. Mueller, A.I. Shoshi, and S.M.H. Wong *Nucl. Phys.* **A762** (2005) 252.
- [53] Y. Hatta, E. Iancu, L. McLerran, and A. Stasto, *Nucl. Phys.* **A762** (2005) 272.